

# Advances in Cell-Rich Inks for Biofabricating Living Architectures

José Almeida-Pinto, Beatriz S. Moura, Vítor M. Gaspar,\* and João F. Mano\*

Advancing biofabrication toward manufacturing living constructs with well-defined architectures and increasingly biologically relevant cell densities is highly desired to mimic the biofunctionality of native human tissues. The formulation of tissue-like, cell-dense inks for biofabrication remains, however, challenging at various levels of the bioprinting process. Promising advances have been made toward this goal, achieving relatively high cell densities that surpass those found in conventional platforms, pushing the current boundaries closer to achieving tissue-like cell densities. On this focus, herein the overarching challenges in the bioprocessing of cell-rich living inks into clinically grade engineered tissues are discussed, as well as the most recent advances in cell-rich living ink formulations and their processing technologies are highlighted. Additionally, an overview of the foreseen developments in the field is provided and critically discussed.

## 1. Introduction

Human living tissues are naturally heterogeneous, being comprised of different cell types and tissue-specific extracellular matrix (ECM) that self-organize into intricate 3D architectures with complex microarchitecture, physiology, biomechanical, and morphogen gradients.<sup>[1]</sup> In these elegant systems, cells actively communicate with each other (cell-to-cell) and their surroundings (cell-to-matrix), resorting to biophysical and biochemical mediators to dynamically regulate biological responses and maintain proper tissue biofunction.<sup>[2]</sup>

Over the years, the scientific community of tissue engineering and regenerative medicine has been striving to engineer artificial organs/tissues that closely recapitulate the fine cellular and architectural features of native human tissues. However, this goal is yet to be achieved as the current technologies are still ineffective

at recapitulating the complex intricacies of native tissues, thus failing at producing suitable tissue/organ analogs.<sup>[3]</sup>

In native tissues, intricate cell-to-cell/matrix interactions are dynamically established to ensure proper cellular organization and tissue homeostasis.<sup>[4]</sup> As effective cell cross-communication takes place in earlier time points of tissue development, cells tightly communicate through different mechanisms, including secretion of signaling factors, establishment of adherens and tight junctions via direct coupling of membrane molecules (e.g., cadherins, integrins), and gap junctions.<sup>[5-7]</sup> While moving in the timeline of tissue development, the cell–cell crosstalk and deposition/remodeling of the extracellular

matrix ultimately leads to the establishment of dynamic cell–matrix signaling events (e.g., cellular mechanotransduction), that are crucial to ensure proper tissue formation and tissue homeostasis.<sup>[4,8]</sup> Considering this, the recapitulation of the cell richness of living tissues is regarded as one of the most critical aspects to be attained when designing/engineering 3D living architectures.<sup>[9]</sup> Such feature is crucial to ensure the establishment of effective cellular cross-communication in early development stages. These are then key to guide tissue morphogenesis and maturation along time, ensuring the biological potential of the designed engineered tissues.<sup>[10]</sup>

Despite varying among different tissues/organs, it is estimated that the cellular density of native human tissues is within the order of 1 to 3 billion cells mL<sup>-1</sup>.<sup>[9,11,12]</sup> However, conventional tissue engineering platforms (i.e., hydrogels, fiber meshes, sponges, etc.) are mainly designed, resorting to cell-free or cell-laden biomaterial-based structures that physically entrap cells within a biomaterial network or via postseeding processes.<sup>[1,13]</sup> As a result, these platforms are often bioengineered with nonbiologically relevant cell densities ( $\leq 1 \times 10^7$  cells mL<sup>-1</sup>).<sup>[9,14,15]</sup> Consequently, the resultant architectures fail to recapitulate critical aspects of native tissues, including self-organization and bioactivity, due to a lack of cell–cell crosstalk.<sup>[13,16]</sup> In light of this, there has been a paradigm shift toward the usage of increasingly biologically relevant cell densities to create living architectures, with new technologies emerging to improve cell density recapitulation. The achievement of high cell densities allows the establishment of improved cell-to-cell communication, resulting in the formation of living structures with tissue-like biofunctionalities and enhanced biological and clinical performance.<sup>[17,18]</sup> For instance, researchers have shown that cardiac tissues engineered

J. Almeida-Pinto, B. S. Moura, V. M. Gaspar, J. F. Mano  
 Department of Chemistry  
 CICECO – Aveiro Institute of Materials  
 University of Aveiro  
 Campus Universitário de Santiago  
 Aveiro 3810-193, Portugal  
 E-mail: [vm.gaspar@ua.pt](mailto:vm.gaspar@ua.pt); [jmano@ua.pt](mailto:jmano@ua.pt)

 The ORCID identification number(s) for the author(s) of this article can be found under <https://doi.org/10.1002/adma.202313776>

© 2024 The Authors. Advanced Materials published by Wiley-VCH GmbH. This is an open access article under the terms of the [Creative Commons Attribution](https://creativecommons.org/licenses/by/4.0/) License, which permits use, distribution and reproduction in any medium, provided the original work is properly cited.

DOI: 10.1002/adma.202313776

with  $4 \times 10^7$  cells mL<sup>-1</sup> exhibit spontaneous beating.<sup>[19]</sup> However, one must take into consideration that, extremely high cell densities can pose major nutrition/oxygenation challenges, ultimately resulting in the necrosis of biofabricated tissue-mimetic architectures.<sup>[17,20]</sup> Therefore, efforts should be directed toward the development of platforms capable of processing optimal high densities suitable for a specific tissue, while mimicking the differences found for each cell type.<sup>[21]</sup> When aiming to fabricate tissue mimetic living constructs with architectural complexity similar to native tissues, biofabrication tools play a critical role in processing high cell densities into spatially defined arrangements.<sup>[9]</sup> 3D bioprinting can be perceived as a fundamental piece in the biofabrication of engineered tissues. It enables the processing of multiple building blocks into precise spatial arrangements with high resolution, showing great potential to generate de novo biomimetic living tissues.<sup>[22]</sup> Exploiting cells as fundamental building blocks for bottom-up engineering places the field one step closer to fabricating tissue-like living architectures.<sup>[13]</sup>

Currently, the processing of such cell-rich inks into tissue-like living architectures remains hampered by numerous challenges (i.e., cell viability, resolution, scale-up, maturation, etc.), hindering the successful processing of cell-rich living inks into living structures with architectural complexity and adequate resolution.<sup>[18,23–25]</sup> Despite the advances made toward the processing of high cell densities (e.g.,  $>2 \times 10^7$  cells mL<sup>-1</sup>), the printing of tissue-like cell densities is still far from being realized, and innovative methodologies are needed to fabricate and process an outstanding number of living building blocks into spatially organized functional structures.

Regarding this, herein we aim to showcase the recent advances in the development of cell-rich inks intended for advanced biofabrication, especially for high-cell-density 3D bioprinting (HCD 3D bioprinting). Throughout this review, we highlight the hot topic challenges that currently hinder the HCD bioprinting field and how the scientific community has been elegantly engineering cell-rich inks with increasingly higher cell densities ( $>2 \times 10^7$  cells mL<sup>-1</sup>), by exploring different living building blocks (unitary cells, spheroids, tissue strands, organoids, etc.). Additionally, we provide a critical overview of the foreseen advances of the field, especially regarding the design of living inks with tissue-like cell densities and advances in bioprinting platforms to eventually generate highly biomimetic 3D engineered tissue/organ analogs able to translate for clinical applications.

## 2. Toolboxes and Challenges for Engineering Cell-Rich Living Inks

Up-to-date, the field has been mostly focused on developing bioink formulations that are inherently rich in biomaterials, while incorporating relatively low cell densities per bioink volume (i.e., high biomaterial-to-cell ratio). While such formulations provide superior printability and higher potential for scalability, such bioinks tend to restrict cellular reorganization within the constructs and limit cell–cell interactions, which directly interferes with the biological maturation of the printed construct (e.g., cell proliferation, scaffold degradation, de novo ECM deposition).<sup>[26–28]</sup> Since material–material cross-linking mechanisms are crucial to the assembly of such cell-laden biomaterial-based structures, the biomaterial-to-cell ratio should be high

enough so that cells do not hinder the cross-linking efficiency. Considering this lack of biomimicry to native tissues, a paradigm shift toward reversing such design (i.e., to high cell-to-biomaterial ratio) has potential to improve the overall biological performance of biofabricated living architectures, by maximizing cell-to-cell communication and improving tissue formation.

Despite the remarkable advances in HCD bioprinting, the development of clinical-grade engineered tissues/organs through the processing of cell-rich inks by advanced biofabrication techniques is still far from being reached. Numerous hurdles remain to be solved and simultaneously combined, including: i) recapitulation of the architectural and organizational complexity of native tissues by addressing aspects such as multicellularity, morphogenic/topologic cues, embedding vascularization, resolution of cell placement, and mechanical robustness; ii) ensuring cytocompatibility and maturation to achieve physiologic levels of biological functionality; iii) quality control and safety standards; iv) supply of cellular materials; among others. Nonetheless, with emerging advances in the scalability and resolution of 3D bioprinting platforms, the biomanufacturing of clinical-grade engineered tissues will eventually become a reality (**Figure 1**).

### 2.1. HCD Biofabrication Platforms

In an attempt to unlock HCD bioprinting, a plethora of widely known biofabrication techniques have been explored over the years to successfully process cell-rich living inks, including droplet-based, extrusion-based, digital light processing (DLP), volumetric bioprinting, Kenzan bioprinting methodology, and aspiration-assisted bioprinting.<sup>[22,25,29,30]</sup> Nonetheless, despite the advances in multiple bioprinting technologies, there are still difficulties in simultaneously processing multiple cell types into specific patterns while ensuring the high resolution and cytocompatibility of the structure.<sup>[23]</sup> Aside from typical drawbacks of each printing technology, when high cell densities are added to the equation, the layer of challenges becomes thicker, hindering the rapid progress of the field. Considering this, huge efforts have been made in the development of new and/or improved technologies to process such high cell densities. These main drawbacks are usually regarded and presented as the density–viability–resolution trilemma of 3D bioprinting, which states the difficulty of simultaneously process relatively high cell densities with high resolution while ensuring high cell viability.<sup>[9]</sup> As already defined in the literature, herein we will be considering a cell density of  $2 \times 10^7$  cells mL<sup>-1</sup> as the baseline for HCD bioprinting.<sup>[9]</sup> Despite covering the current state-of-the-art technologies, this baseline value can strongly vary considering the platforms employed, and certain approaches have already achieved a higher baseline. Following this trend, we may expect that this value will dramatically increase with the advances in biofabrication technologies and living ink formulations, moving toward increasingly higher and more tissue-mimetic cell densities.

Droplet-based bioprinting, such as inkjet-based and microvalve-based technologies, have been widely used for fabricating cell-laden 3D constructs via the deposition of controlled volumes onto predefined regions of a receiving substrate.<sup>[25,31]</sup> Droplet-based strategies offer several advantages, including high cell viability, speed, and accuracy, as well as the possibility to

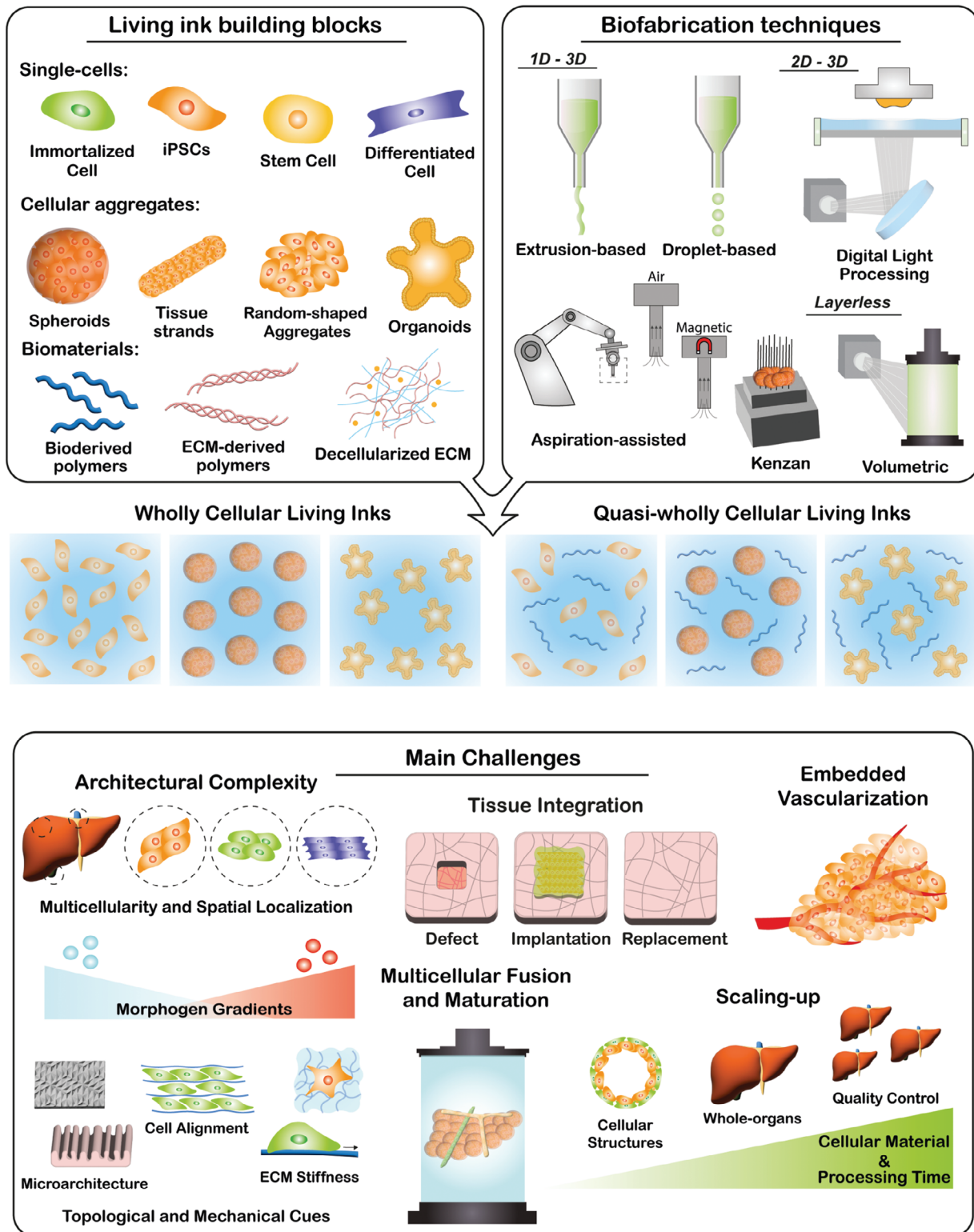


**Figure 1.** Schematic illustration of the representative building blocks used in living ink formulations and their processing under different biofabrication techniques. Upon adequately selecting the living ink composition and respective biofabrication platform, the living inks can be processed to generate living materials. The printing of cell-rich structures and engineered tissues/organs presents multiple challenges imposed by current technologies and ink formulations, including the capability to closely recapitulate the architectural intricacies of native tissues, the need for a properly functional embedded vascularization to ensure tissue viability and functionality, as well as others such as scaling-up problems, tissue integrability, and proper fusion and maturation of the combined building blocks.

introduce gradients by tuning drop densities and sizes.<sup>[25,32]</sup> Despite such advantageous processing properties, droplet-based bioprinting methodologies also suffer from multiple drawbacks. One common limitation is the limited ranges of processable material viscosity (e.g., especially for inkjet-based bioprinting), since the bioink should be in a liquid-like form to enable the formation of droplets and avoid nozzle clogging.<sup>[25,32]</sup> Owing to this, such platform is strongly limited to the incorporation of biomaterials capable of promoting cross-linking of the living inks and generate stable structures. Moreover, to aid in droplet formation, these platforms are usually limited to suboptimal cell densities, far from biologically relevant, where an increment to higher cell densities could also result in an inhibition of cross-linking mechanisms and an increase in viscosity, hindering the translation of such technologies for HCD bioprinting.<sup>[25,33,34]</sup> In general, droplet-based bioprinting presents an appreciable resolution ( $>50\ \mu\text{m}$ ).<sup>[33]</sup> However, this is still far from the desired resolution to respond to the 3D bioprinting trilemma, while aiming for the fabrication of highly biomimetic tissues that recapitulate critical architectural features.<sup>[29]</sup> Besides that, these methodologies are unsuitable for recapitulating significant thickness values, hindering their translation to large-scale engineered tissues.<sup>[29]</sup> Nonetheless, despite the numerous drawbacks of this bioprinting category, which hinders the successful translation to HCD bioprinting, certain research groups have been pushing droplet-based bioprinting toward the printing of increasingly higher cell densities. For instance, a reactive jet impingement platform was successfully developed to print cell densities of  $4 \times 10^7\ \text{cells mL}^{-1}$  with high printing speed and droplet accuracy.<sup>[35]</sup> Additionally, an inkjet-based bioprinting platform resorted to a piezoelectric dispenser, having printed cell-rich inks with  $2.5 \times 10^7\ \text{cells mL}^{-1}$ , leveraging on the resulting cell-dense droplets as building blocks for fabrication of higher order architectures.<sup>[36]</sup>

On the other hand, extrusion-based bioprinting consists of a layer-by-layer deposition of a continuous filament of bioink, loaded with living building blocks onto the desired locations to fabricate 3D architectures.<sup>[34]</sup> Usually, in this modality the living building blocks are commonly combined with a wide range of biocompatible materials, preferably with shear-thinning behavior and cross-link triggers (i.e., light, thermal, chemical) to produce a stable structure.<sup>[33]</sup> A critical advantage of extrusion-based bioprinting over other bioprinting methodologies is its ability and propensity to process high cell densities, attracting great attention as a platform for HCD bioprinting of living inks comprised by a nonlimited range of building blocks. However, this methodology can be unsuitable for high-resolution deposition of the building blocks due to nozzle and extrusion pressure limitations, which strongly impacts cell viability due to the shear stress exerted during the extrusion process.<sup>[37–39]</sup> This impact in cytocompatibility becomes more evident when translating to HCD bioprinting, where an increasing cell density or usage of larger building blocks, such as spheroids, requires the use of larger nozzles (usually  $>200\ \mu\text{m}$ ) to mitigate the shear stresses and ensure high viability and consequently proper tissue functionality.<sup>[33,34]</sup> Such physical limitation results in poor printing resolutions, thus failing to recapitulate the structural complexity of native human tissues, and in slow printing speeds.<sup>[33]</sup> However, resorting to special supporting baths, such difficulties have been mitigated. For instance, living inks have been successfully printed into pho-

toactive microgel slurries, which helps to maintain high print fidelity, allowing the printing of living structures without the incorporation of biomaterials in the ink's formulation to provide integrity.<sup>[40]</sup> Despite this, extrusion-based bioprinting represents a promising platform to urge HCD bioprinting by being capable of processing multiple living building blocks into relatively large living structures.<sup>[17,23]</sup> A synergistic combination with microfluidics may allow the prealignment of the living building blocks prior to the printing process. This approach can drastically reduce the risk of clogging associated with nozzle-based platforms and contribute to mitigating the shear stress in cell-rich inks. Additionally, the exploitation of materials such as microgels and nanoparticles, as ink lubricants may also contribute to the reduction of the shear stress by altering the rheologic properties of the living ink during the extrusion process.

Aside from the “1D-to-3D” printing logic followed by extrusion- and droplet-based bioprinting technologies, light-based bioprinting, including DLP and volumetric bioprinting, rely on the delivery of light into specific locations of a photoreactive ink, either in a layer-by-layer light projection style (“2D plane-to-3D structure” logic) or in a layerless light tomography approach to generate 3D structures.<sup>[9,23]</sup> In contrast to extrusion-based technologies, which present physical limitations that further limit printing resolution, light-based bioprinting is capable of achieving micrometer-scale resolutions, that can even extend to the sub-micrometer scale.<sup>[9,38]</sup> Regarding such precision, these platforms have the potential to recapitulate fine and complex features of native tissues. Despite their potential, the incorporation of increasing cell numbers into the living ink formulations results in a higher light scattering effect, and thus the printing resolution decreases.<sup>[41]</sup> Such effect becomes more pronounced when higher cell densities or high-order building blocks (e.g., spheroids and organoids) are included in living ink formulations, especially due to the increase in the mismatch between the refractive index of cells and the surrounding environment.<sup>[9]</sup> As a consequence, the printing resolution and exploitable cellular densities are limited in these platforms, imposing barriers to a successful high-resolution HCD bioprinting. In suboptimal cell density studies, these effects have started to be mitigated by computational approaches,<sup>[41,42]</sup> or through the incorporation of chemical additives, that are usually cytotoxic for cells.<sup>[43]</sup> However, the incorporation of iodixanol, a biocompatible chemical additive, into a cell-rich ink ( $>1 \times 10^8\ \text{cells mL}^{-1}$ ) successfully allowed researchers to tune the refractive index of the ink, allowing the printing of structures with biologically relevant cell densities and a resolution of  $\approx 50\ \mu\text{m}$ .<sup>[9,44]</sup>

Despite volumetric bioprinting has enabled researchers to achieve higher fabrication speeds when compared to DLP-based techniques, the overall resolution becomes intrinsically more affected by light scattering events, for example, as those related to high cell densities.<sup>[9,41,44]</sup> Owing to this, volumetric bioprinting is currently rather limited when the processing of high cell densities is desired. Nonetheless, despite not achieving yet the cell density baseline herein defined, advancements toward the processing of higher cell densities have been made using this elegant technology. By exploring such technique, researchers were recently able to successfully fabricate complex centimeter-scale liver-like tissues by using a gelatin-methacryloyl (GelMA)-based bioresin, optically tuned with iodixanol.<sup>[44]</sup> Such setup allowed



the processing of hepatic-organoid- and single-cell-based structures, with relatively high cell densities, up to  $1.5 \times 10^7$  cells  $\text{mL}^{-1}$ , paving new ways toward the exploitation of volumetric bioprinting to process increasing cell densities.

Besides the typical bioprinting platforms, new methodologies for HCD bioprinting have been emerging, especially through the processing of cellular aggregates as the fundamental building blocks. In these approaches, Kenzan bioprinting has been highly explored for bioprinting of spheroids in a scaffold-free manner by resorting to a needle array that provides temporary support to precisely position the advanced building blocks.<sup>[30,45]</sup> However, spheroids are subject to physical disruption forces, mandatorily requiring a set of same-sized spheroids to properly fit in the needle array, while at the same time experiencing challenges regarding the z-axis positioning.<sup>[46,47]</sup> Alternatively, resorting to aspiration forces, aspiration-assisted bioprinting (AAB) has also enabled the picking and precise placing of living spheroids with appreciable positioning resolution.<sup>[46,48]</sup> Recently, AAB has been used for bioprinting tissue spheroids via spatial positioning into sacrificial gels, allowing the retrieval of the structure after spheroid fusion and structure maturation.<sup>[46]</sup> Using this strategy, spheroids have been printed into self-healing yield-stress gels, with considerable placement precisions between  $\approx 11\%$  and  $15\%$  with respect to spheroid size.<sup>[46,48]</sup> AAB-based approaches have great potential for addressing common drawbacks found in other biofabrication technologies for processing spheroid-containing cell-rich inks. Nonetheless, aspiration forces may need to be tuned according to the specific surface tension of the building blocks in order to avoid disruption and cell damage.<sup>[49]</sup>

Ideally, engineered living inks should fulfill certain requisites that can match the needs of specific biofabrication platforms, while ensuring cell viability and functionality of the final architectures.<sup>[27]</sup> However, when moving toward HCD bioprinting, implementing/tuning such ink properties becomes ever more challenging (Table 1). Despite the enhanced biological performance of living inks, owing to their high-cell densities, their mechanical/rheological properties may become a limiting factor, thus hindering their processability by widespread biofabrication technologies that are commonly used in the field.<sup>[26,50]</sup> In order to fulfill the needs required for HCD printing, important parameters, including resolution, scalability, cell viability (pre-, during-, and postprinting) and processing speed, should be addressed and improved to evolve the field.<sup>[23]</sup> These may be achieved by improving technical issues of the distinct biofabrication techniques, and/or the tuning of ink's formulation and properties, with the possibility to incorporate minimal fractions of biomaterials, to either act as cross-linking agents or as supportive sacrificial materials, that can provide initial structural integrity while allowing cellular fusion at later stages of maturation.<sup>[51]</sup>

## 2.2. Scale-Up

The successful creation of clinically transplantable large-scale tissues is also strongly limited by the scaling limitations of 3D bioprinting. For instance, an outstanding number of cells are required to be processed as living building blocks in cell-rich inks and to be patterned at the macroscale. Considering that a typical human adult-size solid organ is composed of 10–300 billion cells,

HCD printing of clinically relevant engineered tissues/organs is currently limited by the lack of cellular material.<sup>[11,54]</sup> Furthermore, the amount of cellular material drastically increases if one accounts for the numerous variables that should be considered while designing clinical-grade organs (e.g., quality control, printing parameters, perfusion, or maturation optimization).<sup>[11,23]</sup> Considering this, researchers have proposed a manufacture-to-printer pipeline to provide 3D bioprinting with enough cellular material to include in cell-rich inks formulations for generating large-scale tissues. This manufacture-to-printer pipeline will be critical for the scalable production of viable building blocks to be employed in tissue-scale HCD bioprinting, revealing the importance of automated bioreactors as critical inputs for this emerging field.<sup>[11]</sup> Moreover due to the large amount of ink and bioprinting time required to completely print macroscale tissues/organs, special attention should also be provided to the dehydration of the ink, during the printing process.<sup>[23]</sup>



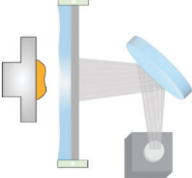
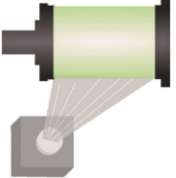
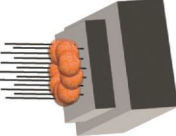
## 2.3. Vascularization and Tissue Oxygenation

Besides the lack of cellular material, macroscale tissue fabrication has also been limited by the absence of engineered vascular networks capable of maintaining the viability of engineered tissues during the maturation process, by providing a continuous supply of nutrients and oxygen, as well as ensuring waste products removal, along the engineered tissue.<sup>[15,23,29,55]</sup> Once tissue volume exceeds the vascularization threshold ( $\approx 1 \text{ mm}^3$ ), the viability starts to decrease due to the lack of an embedding vasculature, thus vascular networks should be simultaneously included during the biofabrication process.<sup>[15,23,56]</sup>

However, the bioengineering of natural-like hierarchically branched and perfusable vasculature networks, that closely recapitulate those found in native tissues, represents a major challenge that needs to be addressed to ensure viable large-scale engineered tissues.<sup>[57]</sup> Resorting to embedded printing methods, such as sacrificial writing into functional tissue, perfusable and branched embedded vasculature has been created by printing a sacrificial ink within a compacted granular organoid bath.<sup>[15]</sup> After organoid fusion and maturation, the sacrificial ink is subsequently removed, leaving a perfusable and branched vascular tree embedded within the engineered tissue of biologically relevant cell densities ( $\approx 2 \times 10^8$  cells  $\text{mL}^{-1}$ ).<sup>[15]</sup> Additional embedding technologies, such as freeform reversible embedding of suspended hydrogels<sup>[58]</sup> have also been explored, as well as the extrusion of living inks comprised uniquely by spheroids to design multilayered and branched tubular structures to mimic the complex features of native tissue vasculature.<sup>[52]</sup> Additionally, the combination of HCD bioprinting with soft microfluidics holds great promise in attempting to recapitulate the dense and branched capillary networks.<sup>[59]</sup>

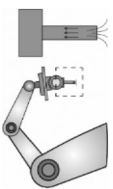
Other strategies may also be explored to ensure the oxygen supply to large-scale engineered tissues. Oxygen-releasing materials (ORMs) have been explored to precisely control the oxygenation of engineered tissues, addressing typical hypoxia-related events, and promoting a higher viability and functionality of the constructs.<sup>[60,61]</sup> The inclusion of oxygen-generating materials (i.e., calcium peroxide (CPO))<sup>[62,63]</sup> or oxygen carriers (i.e., perfluorocarbon compounds)<sup>[64,65]</sup> in living ink formulations may be

**Table 1.** Comparison between key parameters of biofabrication platforms under exploration for HCD bioprinting.

Biofabrication platform	Resolution	Speed	Cell viability	Scalability	Design considerations	Critical parameters	Refs.
 Droplet-based	Low– Medium	Medium	Medium– High	Very low	Ink viscosity Substrate properties Nozzle size Cross-linking mechanism	Limited to the incorporation of biomaterials into ink formulation Possibility of nozzle clogging	[25,31,32,36]
 Extrusion-based	Low– Medium	Low– Medium	Medium– High	Medium– High	Ink viscosity/rheological properties Nozzle size, pressure, and speed of printing Usage/absence of supporting bath	Possibility of nozzle clogging The usage of high pressure may result in high shear stress and affect cell viability Time required to process large constructs may affect cell viability/functionality	[17,23,37,40,52]
 Digital light processing	High	Fast	High	High	Photopolymerization parameters (light penetration, irradiation time, etc.) Refractive index tuning agent selection	Light scattering Possible cytotoxic effects of refractive index tuning agents	[9]
 Volumetric	High	Fast	High	High	Photopolymerization parameters (light penetration, irradiation time, etc.) Bioresin composition Refractive index tuning agent selection	Strong light scattering effects and limited cell density Possible cytotoxic effects of refractive index tuning agents	[9,41,44]
 Kenzan	Medium– High	Low	Medium	Low	Spheroid size Needle array parameters (array configuration and interdistance)	Physical disruption forces Require equally sized spheroids to ensure homogeneous placement and tissue fusion six-axis positioning	[30,45,53]

(Continued)

Table 1. (Continued)

Biofabrication platform	Resolution	Speed	Cell viability	Scalability	Spheroid properties (size and surface tension)	Design considerations	Critical parameters	Refs.
Aspiration-assisted	Medium–High 	Low	High	Low	Spheroid properties (size and surface tension)	Aspiration force Supporting bath	Require equally sized spheroids to ensure homogeneous placement and tissue fusion Physical disruption forces	[46,48,49]

advantageous when aiming toward viable macroscale tissues. For instance, hydrophobic oxygen-generating micromaterials were developed through the encapsulation of CPO in polycaprolactone microparticles.<sup>[66]</sup> The oxygen-generating system allowed a prolonged and controlled oxygen release, leading to a higher production of vascular endothelial growth factor and promotion of proangiogenic hypoxia. Considering this, self-oxygenation systems may potentially improve the survival of large-scale engineered tissues by driving full-thickness vascularization. Nonetheless, despite addressing hypoxia-related problems, such strategies are still regarded as a short-term option since they lack the capability to address the nutritional and waste-clearing needs of macroscale tissues. Thus, the inclusion of ORM in living ink formulations may be a valuable complementary option to assure proper oxygenation and stimulation of vascularization in large-scale constructs, improving the survival rates of engineered tissues during the initial developmental states.<sup>[66]</sup> Advances in other oxygenation platforms, such as electrocatalytic on-site oxygenators, developed to produce and deliver regulated dosages of oxygen locally, hold great promise to sustain cell viability in cell-dense constructs by improving tissue oxygenation.<sup>[67]</sup> Additional strategies arise while exploiting higher-order building blocks, specially coculture with endothelial cells, that allow the development of prevascularized units which can be further combined as building blocks and enhance vascularization of printed constructs.<sup>[28]</sup> Following this rationale, researchers have been combining endothelial and mesenchymal stem cells (MSCs) to generate spheroids that reveal enhanced osteogenic differentiation and angiogenic potential, which were explored for bone tissue bioprinting via AAB.<sup>[68]</sup> Moreover, human-induced pluripotent stem cell derived endothelial cells (ECs) were combined with MSCs and iPSC-derived cortical neural progenitor cells, to study neural–vascular interactions.<sup>[69]</sup> Despite of not achieving mature vascular structures, improvements in the design of prevascularized units are expected to contribute to vascularization of living structures.

Dynamic perfusion culture approaches are also increasingly emerging as a valuable strategy for ensuring long-term survival of cell-dense living constructs, by providing a dynamic and controlled culture environment that homogeneously ensures the supply of nutrients and oxygen, as well as dynamic fluid-flow-associated stimulation, that may help in the development of certain types of tissues (e.g., bone tissue).<sup>[70–72]</sup> In the future, when clinical applications are envisioned, the usage of perfusion bioreactors, allied to advanced vascularization/oxygenation strategies, may contribute to improve the overall cell viability and biofunctionalities of tissue-mimetic constructs.<sup>[70]</sup> In this line of thinking, interesting setups combining volumetric bioprinting and dynamic perfusion have been revealing promising results in the study and enhancement of hepatic functions of the liver-like tissues.<sup>[44]</sup>

#### 2.4. Tissue Maturation and Handleability

Ultimately, the post-HCD bioprinting process requires the successful assembly of the printed smaller living building blocks into mechanically robust high-order living structures with tissue-matched biofunctionalities, capable of maintaining their

integrity during the maturation, handling, and eventually, transplantation processes.<sup>[22,73]</sup> However, in 3D bioprinting of cell-rich inks, normal tissue morphogenesis is bypassed, thus a longer maturation period is required in order to ensure the self-assembly and fusion of the living building blocks into cohesive structures through the formation of native cell–cell and cell–matrix interactions via native cell adhesion molecules (e.g., E-, N-, P-cadherins, integrins, etc.).<sup>[23,25,74–76]</sup> This naturally based cross-linking process is critical to ensure robustness for handling processes and is the most widely found cross-linking process currently explored in HCD bioprinting. Currently, supporting baths are widely exploited to sustain the constructs and maintain their spatial arrangement while the self-assembly process occurs.<sup>[77]</sup> For instance, self-healing hydrogel supporting baths, based on adamantane/cyclodextrin host–guest pair, have been designed to maintain the precise spatial arrangement of spheroids during the deposition, as well as fusion processes.<sup>[47]</sup>

Nevertheless, natural self-assembly processes usually take long periods, which can extend up to several days.<sup>[15,23]</sup> Thus, the design of functional building blocks by resorting to cell engineering techniques may help to speed up the maturation process. By chemically or genetically programming the self-assembly process in a user-defined manner, higher spatiotemporal resolution over the fabrication process may be attained, improving the processability of the engineered tissues.<sup>[109]</sup> This accelerated assembly rationale is still in its infancy, however huge advances have been made toward this aim. By combining metabolic glycoengineering with bioorthogonal chemistry, high-cell-density living materials have been developed by exploiting bioorthogonal reactions between azide moieties displayed at metabolic glycoengineered cells and dibenzocyclooctyne groups in polymeric networks of branched alginate.<sup>[78]</sup> Despite not being yet applied for bioprinting purposes, the injectability of such systems shows great potential, resembling interesting living inks to be explored for HCD bioprinting.<sup>[79,80]</sup>

### 3. Bioprinting Cell-Rich Living Inks

Cell-rich inks play a crucial role in HCD bioprinting, acting as a precursor solution that allows the organization of living building blocks in a precise and controlled manner to fabricate engineered living tissues. Relying on the complexity of the building blocks, the processing of such cell-rich inks can aim for the direct emulation of the anatomical features of native tissues or rely on developmental biology aspects to replicate morphogenesis and organogenesis events and self-organize into an engineered functional tissue. Regarding this, the current living building blocks explored in HCD bioprinting can consist of unitary cells and/or multicellular aggregates, encompassing spheroids, tissue strands, organoids, among other shaped aggregates.<sup>[28]</sup>

Single cells can be perceived as a basic living building block to be explored for HCD bioprinting applications. Importantly the exploitation of individualized cells as building blocks may require longer maturation periods to achieve proper cell fusion and self-organization within the printed constructs, as they are less complex building blocks when compared to multicellular aggregates, invariably lacking prior cellular organization/maturation.<sup>[40,81]</sup> Nonetheless, their exploitation may also result in a more homogeneous fusion within printed constructs.<sup>[82]</sup> On the other

hand, the inclusion of preformed multicellular aggregates (e.g., spheroids, tissue strands, organoids, etc.) in cell-rich inks for HCD bioprinting may offer advantages over unitary cell inks' printing. For instance, the printing of advanced building blocks may result in accelerated tissue maturation through the recapitulation of complex microarchitectures and cell-type diversity of living structures, revealing the potential to fabricate engineered living architectures with tissue- and organ-level functionalities.<sup>[23,25,83]</sup> Moreover, the usage of such multicellular building blocks addresses scaling limitations faced by unitary-cell-based inks, namely by reducing the time required to fabricate whole organs owing to the intrinsic high cell numbers of such multicellular building blocks.<sup>[23]</sup> Regarding this, there is a growing interest in combining complex aggregated building blocks into larger and physiologically relevant engineered tissue-mimetics. However, their usage may also be associated with pre- and postprinting challenges. For instance, multicellular aggregates, such as spheroids and organoids may lead to clogging problems (e.g., in extrusion-based bioprinting), or to variable fusion patterns.<sup>[28,84]</sup> Considering these building blocks, other cellular aggregates, such as tissue strands, have also been fabricated in an attempt to tackle such reproducibility and variability issues, offering evenly shaped multicellular aggregates.<sup>[81,85]</sup> Both types of living building blocks have been paving their way in HCD bioprinting, rendering two distinct living inks categories, namely: i) unitary cell living inks and ii) aggregated cellular living inks, both of which will be showcased in the following subchapters.

It is also relevant to highlight that the inclusion of a biomaterial fraction may be considered when designing living inks. Depending on this, living ink formulations are herein regarded as “wholly cellular” inks, when comprised entirely by these living building blocks, or “quasi-wholly cellular” inks, when biomaterials are included. Wholly cellular living inks have been emerging in the field of HCD bioprinting, resorting to both single cells and cellular aggregates as building blocks. Their exclusive cellular composition renders printed structures with improved cell–cell interactions, which in turn prompts enhanced ECM deposition, tissue maturation, cell differentiation, among others, closely mimicking native tissues' developmental stages.<sup>[47,86]</sup> However, owing to its “scaffoldless” nature, the resultant structures tend to present low structural integrity, requiring long maturation times to allow cell fusion via intercellular adhesion molecules, and further ECM deposition to confer proper integrity and robustness.<sup>[87]</sup> Advancements have been also made toward the design and processing of quasi-wholly cellular formulations. A wide range of biomaterials have been explored for bioprinting applications, including natural polymers (e.g., collagen, hyaluronic acid, etc.), as well as more complex materials, such as decellularized extracellular matrix.<sup>[88,89]</sup> Ideally, in order to boost the biomimicry level of the printed structures, the material fraction should mimic the heterogeneity of native tissues' extracellular matrix, or at least, be part of its composition, in order to improve cellular proliferation and functionalities.<sup>[90]</sup> Herein, minimal fractions of biomaterials are exploited to promote the stabilization of the printed living structures through cross-linking mechanisms, quickly generating structures with structural integrity instead of relying solely in the relatively slow establishment of intercellular adhesions and production of ECM, as found in wholly cellular counterparts. Aside from cross-linking



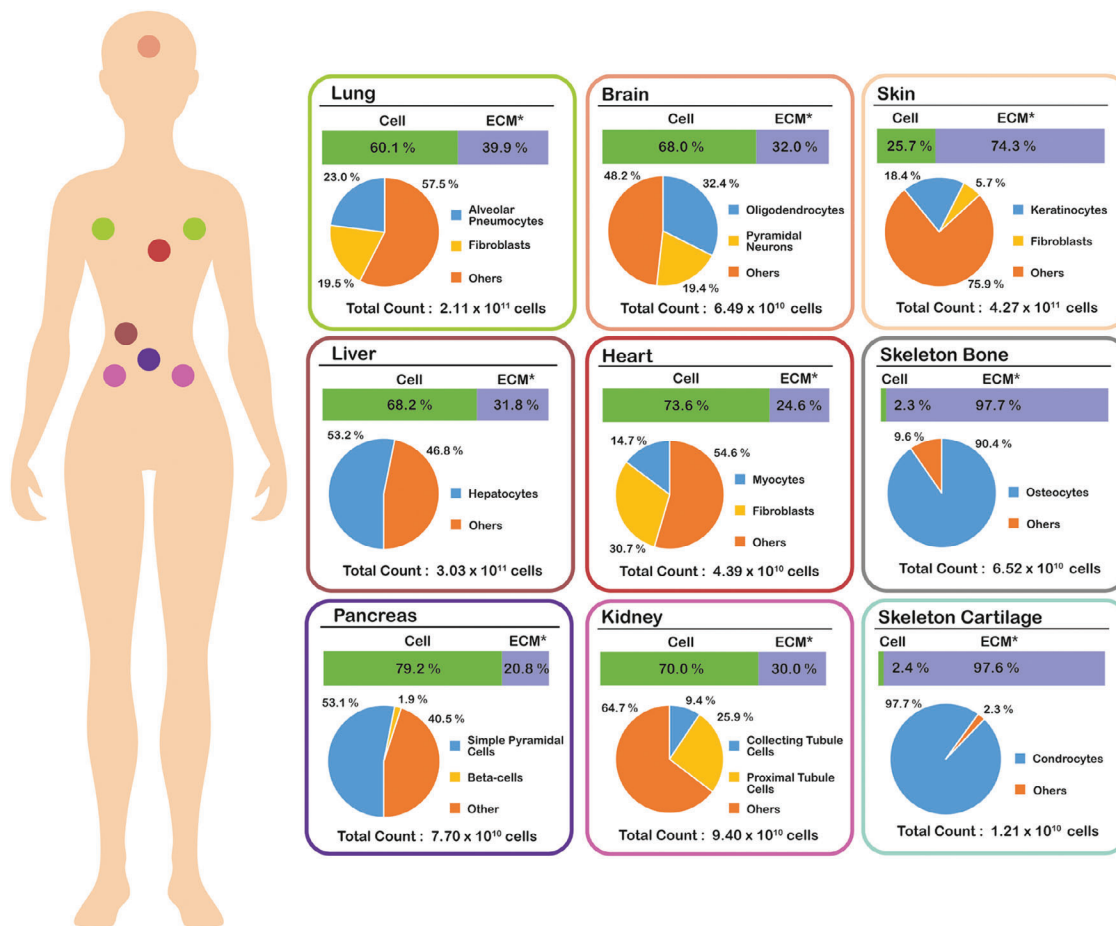


**Figure 2.** Human tissue-specific cell/ECM ratios and cellular profile evaluation. Data were collected from a single study and the corresponding web tool (<https://humancelltreemap.mis.mpg.de>), covering different tissues, including lung, liver, pancreas, heart, kidney, brain, skin, skeleton bone, and cartilage.<sup>[93]</sup> \*ECM portion was estimated by subtracting the total cellular mass from the total tissue weight.

purposes, the inclusion of biomaterials into the inks' formulation may also potentiate the overall ink processability and biological performance of the resultant architectures. For instance, certain printing strategies, such as extrusion-based, may benefit from the inclusion of a minimal fraction of biomaterial, allowing the tuning of the mechanical properties of living inks, in order to ensure higher resolutions, or to act as lubricating agents, ensuring a higher cell viability by reducing shear stress imposed, for example, during extrusion bioprinting. However, the inclusion of exogenous materials in living inks may present inherent limitations, including potential immunogenic responses, unsynchronous biomaterial degradation during tissue formation/repair, as well as the possibility to hinder cell–cell communication, which consequently slows tissue fusion and nascent ECM deposition.<sup>[40,57,91]</sup> In this regard, the exploitation of sacrificial materials have found interesting applications in the field, by providing initial support to the structures, without strongly affecting cellular crosstalk, and, further cellular fusion and ECM deposition.<sup>[92]</sup>

In the near future, while designing cell-rich living inks, researchers should also consider the variability in cell/ECM ratio, cellular heterogeneity, and ECM composition among different

tissues/organs, to design living structures that closely mimic a targeted tissue.<sup>[90,93]</sup> Considering this, we compiled curated information regarding estimated cell/ECM ratio, total cell count, and main cell types of different human tissues (**Figure 2**). Such analysis may provide a road map for designing living inks suitable for specific tissues.

By combining different living building blocks and promoting their assembly, the scientific community has been able to engineer more robust and biomimetic engineered living tissues, with appreciable cell densities and functionalities. Considering this, in the following chapter, we will showcase the most recent advances in bioprinting of cell-rich inks (unitary-cell- and cellular-aggregate-based) exploiting the different cellular building blocks previously mentioned, as well as the bioprinting platform and assembly modes explored to drive their organization into cell-rich engineered living tissues.

### 3.1. Unitary Cell Living Inks

Cells are the basic building block of native tissues, where they self-organize during morphogenesis and organogenesis events

to generate sophisticated hierarchical living structures with complex microarchitectures and cellular arrangements.<sup>[1]</sup> For instance, HCD bioprinting can aim to directly recapitulate the adult tissue anatomy by resorting to unitary cell living inks to precisely place multiple cell types into specific spatial configurations, generating an engineered tissue. However, due to the previously described limitations faced by current bioprinting platforms, the direct anatomical recapitulation of tissue cellular and architectural features, including cell-type diversity and its sophisticated microarchitecture, is still a huge challenge. Nonetheless, significant progress has been made on the processing of unitary cell inks for HCD bioprinting. For instance, wholly cellular inks comprised of multiple human cell types, including adipose-derived mesenchymal stem cells (hASCs), mesenchymal stem cells (hMSCs), and dermal fibroblasts (hDFs) were extruded directly into an oxidized and methacrylated alginate (OMA) microgel slurry, that acts as photocurable liquid-like supporting bath (Figure 3A).<sup>[40]</sup> The properties of the supporting medium allowed the printing of high cell densities with varying printing resolutions according to microgel size, revealing that smaller microgels resulted in higher resolution of the printed filaments. Moreover, after cross-linking, the supporting bath provided sufficient mechanical stability to maintain the fabricated living filaments during long-term culture (i.e., up to 4 weeks) and for osteogenic/chondrogenic differentiation. Thus, the presence of supporting baths can take a critical role in providing support during printing and the maturation process, especially in the case of wholly cellular inks based in unitary cells, that rely only on intercellular interactions. Quasi-wholly cellular inks comprised of human umbilical vein endothelial cells (HUVECs) resuspended in gelatin methacryloyl and iodixanol were also recently printed with a cell density of  $1 \times 10^8$  cells mL<sup>-1</sup> by using DLP bioprinting, generating structures with a considerable high resolution and that showcase the ability of iodixanol to tune light scattering and improve the printing resolution (Figure 3B).<sup>[9]</sup> Additionally, to study the viability of the printed living constructs in a perfusion culture system, a thick and prevascularized engineered tissue was fabricated by combining HUVECs and hDFs in the ink formulation, reaching a combined cell density of  $4 \times 10^7$  cells mL<sup>-1</sup> ( $2.3 \times 10^7$  and  $1.7 \times 10^7$  cells mL<sup>-1</sup>, respectively). After 14 days, endothelialization and angiogenesis were evaluated, and the printed living architectures remained stable and perfusable even after harvesting. Despite the lower handleability when compared to the previous structures, in the same study, living inks containing outstanding cell densities, in the order of  $2.25 \times 10^8$  cells mL<sup>-1</sup>, were successfully printed as softer cylindrical structures, showing exciting results toward the processing of higher tissue-mimetic cell densities by using this platform.

The generation of vascular structures resorting to the printing of cell-rich inks has also been performed by droplet-based bioprinting. For instance, quasi-wholly cellular inks comprised of endothelial cells, including HUVECs and human dermal microvascular endothelial cells (HDMECs), resuspended in fibrinogen, to attain a cell density of  $2.5 \times 10^7$  cells mL<sup>-1</sup>, were successfully processed by this printing platform (Figure 3C).<sup>[36]</sup> Resorting to a piezoelectric dispenser, the cell-dense droplets were dispensed into collagen I and fibrin hydrogel matrices, and consequently acted as building blocks capable of self-assembly and

remodeled the surrounding matrix to generate perfusable lumen-like structures capable of undergoing sprouting and outgrowing small capillaries. Consequently, such a platform revealed great potential to recapitulate the hierarchical branched morphology of vascular networks found in native tissues. On the other hand, new droplet-based printing methodologies have been developed for processing high cell densities. For instance, a new system called reactive jet impingement was developed to print quasi-wholly cellular inks for bone tissue fabrication.<sup>[35]</sup> Resorting to a double microvalve system, the droplets of individual solutions fused in midair, forming a gel before reaching the bioprinter stage. Such platform allowed the simultaneous jetting of droplets of two distinct solutions, namely a i) thrombin and calcium chloride (CaCl<sub>2</sub>) solution containing human telomerase reverse transcriptase-immortalized bone marrow mesenchymal stem cells (hTERT-BMSCs) (cellular component), and a ii) collagen–alginate–fibrin pregel (biomaterial component). This platform allowed an individual printing parameter optimization for each solution, enabling the rapid and accurate fabrication of structures with  $4 \times 10^7$  cells mL<sup>-1</sup>, that remained viable after 14 days in culture in osteogenic medium. Moreover, this study pointed out that the rate of bone formation is strongly correlated with cell density, proving the importance of setting up robust cellular interactions for achieving physiomimetic tissue biofunctionality.

### 3.2. Cellular Aggregate Living Inks

From a different perspective, the biofabrication of engineered tissues can also leverage on developmental biology aspects, through the recapitulation of morphogenesis and organogenesis events. Regarding this, the exploitation of preformed cellular aggregates (e.g., spheroids, tissue strands, and organoids) as advanced building blocks to formulate aggregated cellular inks has attracted great attention of the scientific community, since these higher-order building blocks already present a certain degree of complexity and organization, being capable of self-assembly into scalable and complex tissues.<sup>[27,57]</sup>

Among cellular aggregates, spheroids constitute an attractive living building block, presenting intrinsically enhanced physiological properties and internal cellular organization inherent to the native tissues' cellular arrangements.<sup>[36,94,95]</sup> When spatially placed close to each other, in a permissive environment, spheroids are capable of undergoing postprinting remodeling and fusion. Additionally, spheroids with different maturation stages can be achieved by resorting to bioreactors, allowing the formulation of living inks with maturation heterogeneity. Thus, such advanced building blocks are capable of recapitulating developmental biology aspects and self-organize into robust living structures with their self-produced extracellular matrix.<sup>[45,57,96]</sup> Different bioprinting modalities for processing spheroid-containing inks have been reported in the literature, including extrusion-based, Kenzan, and aspiration-assisted bioprinting.<sup>[45,46,97]</sup> For instance, leveraging on aspiration-assisted bioprinting, researchers demonstrated to successfully pick spheroids assembled from multiple cell types, including, HUVECs and MSCs, into place them in an alginate-based sacrificial gel, acting as supporting bath.<sup>[46]</sup> Resorting to this



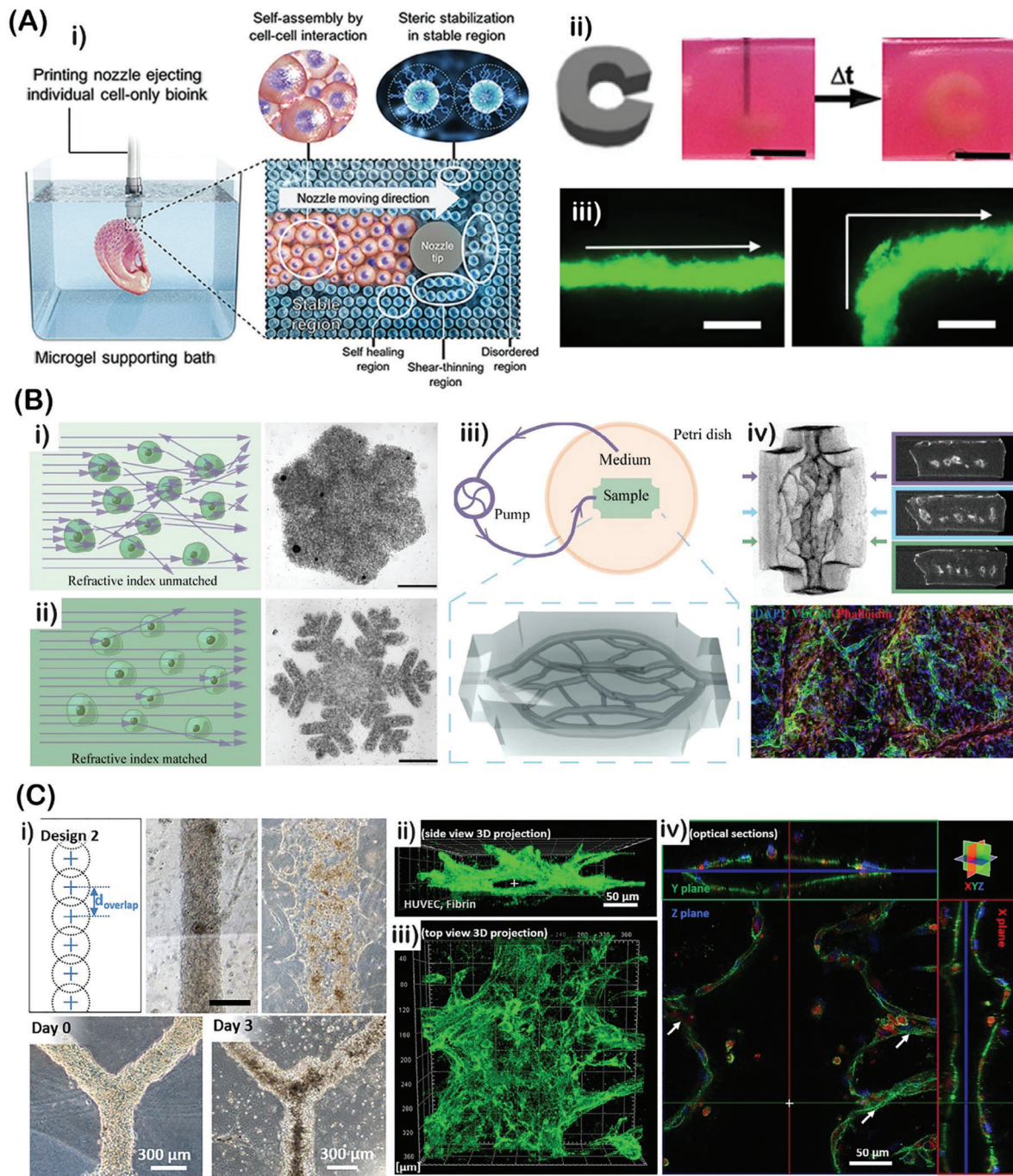


**Figure 3.** Processing of unitary cell living inks. A) Bioprinting of human-based wholly cellular living inks. i) Schematic illustration of 3D bioprinting of wholly cellular living inks into a self-healing and shear-thinning alginate-based microgel (OMA) supporting bath. ii) Digital sketch and optical photographs of the bioprinting process of 3D living constructs. Scale bars: 5 mm. iii) Live/dead staining of printed living filaments with low diameter distribution. Scale bar: 600  $\mu\text{m}$ . Reproduced with permission.<sup>[40]</sup> Copyright 2019, Royal Society of Chemistry. B) DLP bioprinting of highly cell-dense living inks. i, ii) Schematics and optical images comparing living inks with (i) unmatched and (ii) matched refractive index. Scale bar: 600  $\mu\text{m}$ . iii) Schematics of the perfusion system and the digital sketch of the desired vascularized engineered tissue. iv) Microcomputed tomography ( $\mu\text{CT}$ ) of 3D bioprinted vascularized engineered living constructs and respective fluorescence microscopy image of horizontal sections of the channels. Reproduced under the terms of the CC-BY Creative Commons Attribution 4.0 International License.<sup>[9]</sup> Copyright 2023, The Authors, Published by American Association for the Advancement of Science. C) Droplet-based bioprinting of cell-dense vascular structures. i) Schematics of overlapping cell-dense droplets and bright-field images of the resultant continuous and Y-patterned bioprinted structures comprising endothelial cells. Scale bars: 250 and 300  $\mu\text{m}$ . ii, iii) Confocal laser scanning microscopy (CLSM) images of 3D reconstructions of (ii) side and (iii) top view of the bioprinted endothelial-based structures. Scale bar: 50  $\mu\text{m}$ . iv) CLSM images of optical sections of the printed vascular structures in multiple planes. Scale bars: 50  $\mu\text{m}$ . Adapted with permission.<sup>[36]</sup> Copyright 2019, John Wiley & Sons, Ltd.

methodology, spheroids were successfully combined into multiple cell-rich constructs, including rings, pyramids, and diamond-shaped architectures, achieving a positional accuracy of  $\approx 15\%$  relative to spheroid size. The sacrificial gel allowed to maintain the spatial arrangement of spheroids until they became partially fused upon 48 h in culture. Afterward, the sacrificial gel could be carefully removed, and the freestanding structures were cultured in osteogenic media to study the role of midterm osteogenic induction of stem-cell-based spheroids in their assembly behavior for fabricating osteogenic tissues in a bottom-up manner. After proving the potential of such methodology in the bioprinting and assembly of spheroids in a hierarchical manner, researchers decided to aim for the improvement of the general structure properties.<sup>[48]</sup> For this, taking advantage of a sacrificial supporting bath consisting of yield-stress and self-healing gels of Carbopol and alginate microparticles, hMSC spheroids were precisely placed to generate complex living structures, including cartilage and bone tissues (**Figure 4A**). Expanding upon this approach, other supporting baths with interesting properties have been explored. For instance, MSCs spheroids and heterotypic spheroids of human cardiac fibroblasts (hCFs) and hiPSC-derived cardiomyocyte spheroids, combined at different ratios, were picked and precisely placed into a shear-thinning and self-healing supporting bath comprised of adamantane-hyaluronic acid and cyclodextrin-hyaluronic acid (**Figure 4B**).<sup>[47]</sup> Resorting to this technique and to the dynamics of host-guest interactions, individual spheroids were spatially arranged into different shapes, including multilayered rings, capable of maintaining their spatial configuration during fusion and maturation, until being harvested. Then, this concept was leveraged for the fabrication of cell-dense tissue models of post-myocardial-infarction scarring, where hiPSC-derived cardiomyocytes and CF spheroids were printed into the same supporting bath to recapitulate the local heterogeneity and dysfunctions, including reduced contractility and abnormal electrical activity. Despite the challenges of spheroid bioprinting by extrusion-based platforms, this platform remains widely explored for the processing of this building block. Nonetheless, conventional extrusion-based methodologies use bioinks formulated with a higher fraction of biomaterial relative to spheroid numbers. Aiming for HCD bioprinting, living inks for extrusion-based methodologies should be formulated resorting to spheroid slurries, comprised only of spheroids, or a relatively low fraction of biomaterial, to attain high cell densities. Regarding this, wholly cellular inks comprised of human umbilical vein smooth muscle cell (HUVSMC) and human skin fibroblast (hSF) spheroids were extruded into a collagen-based supporting bath (**Figure 4C**).<sup>[52]</sup> Interestingly, resorting to pellets, equally sized spheroids were previously produced by cutting extruded cell-rich cylinders and by letting the fragments incubate overnight until achieving the spherical form. The resulting spheroid-based ink was processed into small-diameter multilayered tubular grafts, revealing great potential for vascular reconstruction. However, the resulting structures required longer fusion times and presented certain nonuniform regions. This troubleshooting led the authors to exploit other cellular aggregate shapes as building blocks, namely strands generated from extruded cell pellets, which resulted in faster fusion rates with higher uniformity. Such prior formation of spherical- and cylindrical-shaped structures resorting to extrusion of cell pellets,

provides a more reproducible strategy to obtain the aggregated building blocks with higher uniformity. Recently, researchers have been exploring prevascularized multicellular spheroids of HUVECs and hMSCs, as living building blocks and combine them with GelMA and fibrin to generate a quasi-wholly cellular living ink (**Figure 4D**).<sup>[98]</sup> Owing to their granular nature, such living ink presents great printing properties that can match those found in jammed microgel bioinks. Upon extrusion, the ink can undergo a double cross-linking, namely photo- and enzymatic-cross-link, resulting in structures with cell densities up to  $1.5 \times 10^8$  cells mL<sup>-1</sup> capable of promoting angiogenesis and undergoing osteogenesis.

Owing to possible size variability and harvesting challenges, researchers have been designing new building blocks that attempt to tackle these issues. Following this rationale, tissue strands have been designed and shown as an alternative to improve the assembly and fusion process of printed structures.<sup>[84]</sup> For instance, centimeter-scale tissue strands comprised by chondrocytes were successfully processed through extrusion-based bioprinting and printed without the need of support baths or delivery materials during the printing process.<sup>[81]</sup> Importantly, such goal may be difficult to achieve while processing other cellular aggregates, including spheroids and strands/cylinders derived from cell pellets, and thus, tissue strands may contribute to improve the scalability of multicellular aggregates as building blocks. The resultant tissue strands revealed rapid fusion, that started 12 h after contact between strands, originating cartilage-like tissues that were further explored in ex vivo osteochondral tissue defects.

The printing of organoid-based living inks can open new possibilities in HCD bioprinting of clinically relevant tissues. Organoids resemble the pinnacle of advanced building blocks, displaying outstanding levels of functionality and structural complexity, closely resembling native tissues in terms of structural complexity and functionality, as well as showing superior biocompatibility, tissue integration, maturation, and regenerative potential, when compared to other building blocks.<sup>[29,83,99]</sup> Nonetheless, bioprinting of preformed organoids is poorly developed and underreported, thus the main approaches center around printing of stem cell aggregates that undergo organoid formation postprinting. Regarding this, high numbers of human induced pluripotent stem cells were generated in the form of aggregates with monodisperse diameters and maintaining pluripotency marker expression (>94%) recurring to automated bioreactors.<sup>[11]</sup> Relying on this scalable manufactory-to-printer pipeline, the pluripotent aggregates were then processed by extrusion-based bioprinting as a wholly cellular ink, with interesting properties, including yield stress, viscoelasticity, and shear thinning, and deposited into a collagen-Matrigel supporting bath. Moreover, since the pluripotency was maintained during serial passaging in the bioreactors, printed pluripotent structures were able to undergo neuroepithelium and vascular organoid differentiation, depending on the differentiation protocols applied (**Figure 5A**). Overall, the combination of scalable platforms with pluripotent aggregates as advanced building blocks proved to be effective in the production of biologically relevant engineered tissues. Nonetheless, the bioprinting of already differentiated aggregates into mature tissues or organoids, prior to bioprinting, would expand the library of building blocks available and may



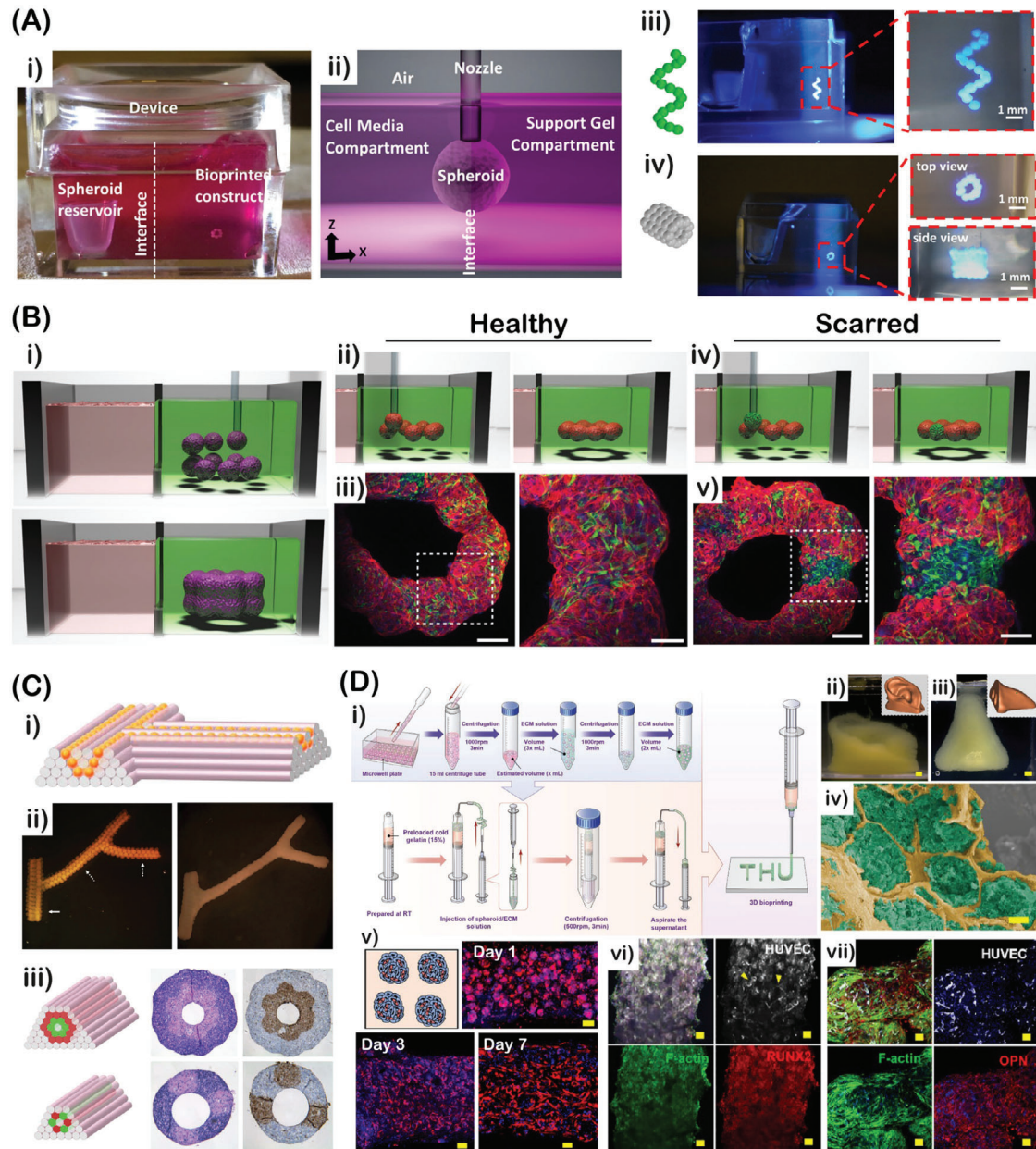


**Figure 4.** Processing of spheroid-based cellular living inks. A) Processing of MSC spheroids into complex hierarchical structures via AAB. i) AAB bioprinting setup showcasing spheroid reservoir and bioprinting compartment. ii) Schematics of the spheroid pickup by a nozzle via aspiration forces. Digital sketch and optical photographs of iii) helix-shape and iv) tubular-spheroid-based structures through 3D bioprinting of MSC spheroids into yield-stress supporting bath. Scale bar: 1 mm. Reproduced under the terms of the CC-BY Creative Commons Attribution 4.0 International License.<sup>[48]</sup> Copyright 2020, The Authors, Published by Springer Nature. B) i) Schematics demonstrating the bioprinting and fusion of spheroids within self-healing support baths. ii–v) Schematics and immunofluorescence images of (ii, iii) healthy and (iv, v) scarred cardiac microtissues comprised of fused spheroids. Red channel – Cardiac troponin-T (cTnT). Green channel – Vimentin. Scale bars: 100 and 50  $\mu\text{m}$  (for insets). Reproduced under the terms of the CC-BY Creative Commons Attribution 4.0 International License.<sup>[47]</sup> Copyright 2021, The Authors, Published by Springer Nature. C) Extrusion bioprinting of vascular structures resorting to spherical and cylindrical multicellular aggregates. i) Schematic illustration of a branched tubular structure comprising multicellular spheroids extruded along with agarose rods. ii) Fluorescence stereomicroscope images revealing fusion of printed hSF spheroids into branched vascular-like structures. iii) Schematics and microscope images of heterogeneous tubular structures obtained from the combination of HUVC and hSF cylindrical-shaped aggregates. Reproduced with permission.<sup>[52]</sup> Copyright 2009, Elsevier. D) i) Schematics of the preparation of prevascularized-spheroid-based living ink combining hMSC and HUVECs. ii,iii) Optical photographs of an ear and nose model bioprinted in a Carbopol-based suspension bath. Scale bar: 2 mm. iv) Scanning electron microscopy (SEM) micrograph of a honeycomb-like bioprinted structure of the quasi-wholly cellular-spheroid-based living ink. Scale bar: 20  $\mu\text{m}$ . v) Schematics and confocal microscopy images of the printed living inks comprised by prevascularized MSC spheroids. Red channel – Red fluorescent protein labeled HUVECs. Blue channel – nuclei. Scale bar: 100  $\mu\text{m}$ . vi,vii) Immunofluorescence images of osteodifferentiated-spheroid-based printed structures analyzed on (vi) day 17 for RUNX2 and (vii) day 24 for osteopontin. Scale bars: 100  $\mu\text{m}$ . Reproduced with permission.<sup>[98]</sup> Copyright 2023, American Chemical Society.

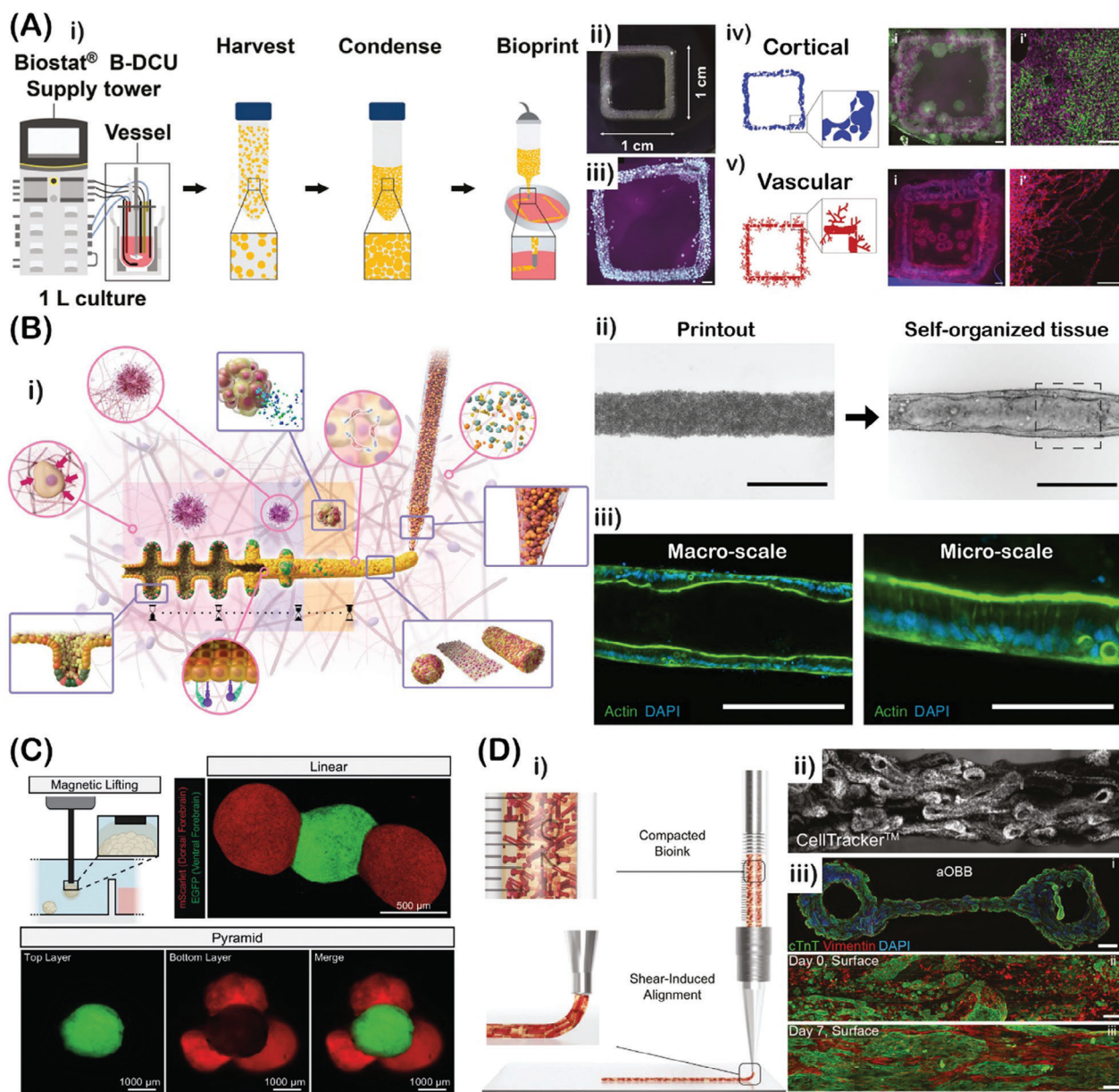


**Figure 5.** Bioprinting of organoid-related and other shaped building blocks. A) Extrusion bioprinting of hiPSC aggregates for cortical differentiation. i) Schematic illustration showcasing stem cell aggregates production and processing into wholly cellular living inks. ii) Optical photograph of a bioprinted square comprised of stem cell aggregates. iii) Fluorescence images of the bioprinted squares from SCVI-15 aggregates immunostained for pluripotency markers. Green channel – OCT4. Magenta channel – NANOG. Scale bar: 1000  $\mu\text{m}$ . iv) Immunofluorescence images showcasing differentiation into neuroepithelium tissue, analyzed at day 10 after the printing process. Green channel – Nestin. Magenta channel – PAX6. Scale bar: 1000 and 100  $\mu\text{m}$  (inset). v) Immunofluorescence images showcasing differentiation into vascular tissue, analyzed at day 10 after the printing process. Red channel – Vascular endothelial (VE)-cadherin. Scale bar: 1000 and 100  $\mu\text{m}$  (inset). Reproduced under the terms of the CC-BY Creative Commons Attribution 4.0 International License.<sup>[11]</sup> Copyright 2022, The Authors, Published by Wiley-VCH GmbH. B) i) Illustration of the processing of intestinal stem cells and organoids under bioprinting for intestinal tissue engineering. ii) Bright-field images of a filament of hiSCs after extrusion, that self-organizes into a connected and polarized epithelial tube. Scale bars: 500  $\mu\text{m}$ . CLSM images showcasing architectural intricacies at the macro- and microscale of the previously organized intestinal tissue. Scale bars: 250 and 75  $\mu\text{m}$ , respectively. Reproduced with permission.<sup>[82]</sup> Copyright 2021, Springer Nature. C) Schematics of magnetic lifting of magnetic-coated human forebrain organoids via magnetic-assisted aspiration-based bioprinting. Fluorescence image from a linear and a pyramidal construction combining dorsal (red) and ventral (green) forebrain organoids to generate neural assembloids. Scale bars: 500 and 1000  $\mu\text{m}$ , respectively. Reproduced under the terms of the CC-BY Creative Commons Attribution 4.0 International License.<sup>[100]</sup> Copyright 2023, The Authors, Published by Springer Nature. D) Processing of complex-shaped cellular aggregates. i) Schematics of processing and alignment of the cardiac anisotropic organ building blocks (aOBBs) during the extrusion-based 3D bioprinting process. ii) Fluorescence images of aOBB within the printed filament, showcasing alignment at the centimeter-scale. Scale bar: 2 mm. iii) CSLM images of aligned aOBBs within the extruded cardiac filaments. Scale bars: 1 mm and 100  $\mu\text{m}$ . Green channel – cTnT. Red channel – Vimentin. Reproduced with permission.<sup>[85]</sup> Copyright 2022, Wiley-VCH GmbH.



be beneficial for HCD bioprinting of more clinically relevant tissues. For instance, researchers attempted the direct printing of human intestinal organoids through extrusion-based bioprinting to produce large-scale constructs capable of undergoing fusion and self-organization.<sup>[82]</sup> However, by employing small intestinal organoids as building blocks, the resultant tubular structures suffered from discontinuous and variable diameters. As hypothesized by the authors, this may be due to the absence of condensation events found in single-cell-based approaches. In light of this, by exploring the organoid-formation potential of human intestinal stem cells (hISCs), the researchers were able to achieve properly connected and polarized epithelial-like tubular structures with high cell densities ( $5 \times 10^7$  cells mL<sup>-1</sup>), mimicking self-organization events of conventional hISC-derived organoids (Figure 5B).

Nonetheless, the direct printing of organoids as building blocks has been successfully materialized by resorting to emerging aspiration-assisted platforms. For instance, researchers developed a new platform that leverages aspiration-assisted bioprinting and magnetic iron-oxide nanoparticles to precisely control the organoid deposition without compromising their cytoarchitecture (Figure 5C).<sup>[100]</sup> In this platform, termed spatially patterned organoid transfer, human forebrain organoids were individually coated with a cellulose nanofiber ink containing iron-oxide nanoparticles and then lifted resorting to a magnetized aspiration-based printer. This platform allowed the precise position of intact organoids to fabricate dorsal–ventral forebrain assembloids, revealing to be a suitable strategy for controlling the spatial configuration of organoids and to generate larger-scale constructs.

Cellular aggregates with more complex shapes have also been explored as building blocks to include in aggregated cellular ink's formulations. For instance, cardiac microtissues were first generated by co-culturing human neonatal dermal fibroblasts (hNDFs) with hiPSC-derived cardiomyocytes (hiPSC–CMs) into micropillar arrays to generate anisotropic building blocks.<sup>[85]</sup> After contraction, the anisotropic building blocks were harvested and combined with a warmed gelatin solution to generate a quasi-wholly cellular ink. Afterward, the ink's extrusion process allowed the alignment of the anisotropic building blocks owing to extrusion forces, resulting in aligned tissues (Figure 5D). Resorting to such methodology, the authors were able to simultaneously recapitulate critical architectural features, namely the aligned phenotype of cardiac tissue, while achieving an outstanding density of  $2 \times 10^8$  cells mL<sup>-1</sup>, after the melting of the sacrificial gelatin layer.

Nonetheless, a few challenges remain to be addressed regarding the production of cellular aggregates as building blocks. Besides the challenges faced by current bioprinting platforms in terms of the processing of such building blocks, the lack of reproducibility and predictability of organoids' formation upstream, as well as, the low shape control, are still hindering their scalable and reliable production for downstream large-scale biofabrication of engineered tissues.<sup>[83,101,102]</sup> Additionally, the standardization of spheroids size is also critical to improve their processing by the current bioprinting platforms.<sup>[30,57]</sup>

We summarized the main examples found in the literature regarding the fabrication of cell-rich living inks and respective target tissues and platforms, as well as other important features, and present them in the following **Table 2**.

## 4. Outlook and Future Perspectives

Despite the biofabrication of clinically translatable tissue architectures being still an unmet reality, huge advances have been recently made in the field of 3D processing of cell-rich inks into large-scale living structures with biologically relevant cell densities and tissue-like functionalities. However, recapitulating key aspects, including spatial organization, vascularization and/or tissue oxygenation, tissue maturation and scale, is still fundamental for the successful fabrication of clinically translatable tissues/organs that simultaneously recapitulate physiological dimensions and biofunctionalities of native tissues.<sup>[44,104]</sup> Although challenging, advancements in bioengineering have been clearly benefiting the HCD bioprinting field, showing exciting progress toward the mastering of such critical and intricate features. In fact, a consensus is still yet to be achieved relating to the degree of biomimicry and architectural complexity required for developing clinically translatable tissues/organs.<sup>[44]</sup> From a cellular perspective, while moving toward the processing of biologically relevant cell densities, the enhanced cell–cell interactions can trigger bioencoded tissue morphogenesis and microarchitectural features, which allied with the spatial placement of biofabrication platforms that may unlock the potential to fabricate increasingly physiomimetic constructs. From a biofabrication perspective, technological evolution toward the precise placement of single cells/cell aggregates, allied with computational simulations/artificial intelligence could provide means to design engineered tissues with programmable microarchitecture and biomechanics that directly recapitulate the complexity of native tissues. New bioprinting techniques have been capable of achieving single-cell precision, allowing the precise selections and positioning of mammalian cells.<sup>[105]</sup> Advancements in such precise techniques may allow a better reconstruction of the complex multicellular configurations found in native tissues, moving toward the fabrication of increasingly complex engineered tissues.

During tissue development, cells intricately move in space or undergo differentiation within precise and defined locations, in a time-coordinated manner.<sup>[106]</sup> Such “life-like” features may also be found in HCD constructs as their behavior will be inherently governed by cells rather than the biomaterial component, as found in the majority of conventional tissue engineered constructs. Recent discussions on morphogenesis and biological pattern acquisition in living tissues could be highly relevant to account for future designs of HCD constructs, especially considering the relevance of biological/chemical gradients in cellular spatial organization within tissues. Gathering inspiration from natural processes, at early design stages, one can envision to imprint relevant shape-morphing features in constructs, in a mode that more closely resembles those found in living tissues.<sup>[104,107,108]</sup> Recapitulating such spatially encoded differentiation may be valuable to recreate complex living tissues, especially by exploring organoids as living building blocks, owing to their physiomimetic potential as they naturally bioencode multicellular diversity and precise spatial organization.<sup>[76]</sup> Additional contributions from genetic engineering and cell surface engineering tools may improve the current knowledge and allow the fabrication of living constructs with user-encoded tissue patterns.

**Table 2.** Summary of main examples regarding cell-rich living ink formulations and respective biofabrication platforms for HCD.

Tissue	Building block	Cell types	Ink type	Cell density	Biomaterial	Biofabrication platform	Supporting bath	Ref.
Bone	Single cell	hASCs; hMSCs; hDFs	Wholly cellular	n.s.	No	Extrusion-based	Methacrylated oxidized alginate microgels	[40]
	Single cell	hTERT-BMSCs	Quasi-wholly cellular	$4 \times 10^7$ cells mL <sup>-1</sup>	Thrombin and CaCl <sub>2</sub>	Droplet-based (reactive jet impingement)	No	[35]
Bone and cartilage	Spheroids	hMSCs; HUVECs	Wholly cellular	n.s.	No	Aspiration-assisted	Alginate	[46]
	Spheroids	Immortalized hBMSCs	Wholly cellular	n.s.	No	Kenzan	No	[53]
	Spheroids	HUVECs and hMSCs	Quasi-wholly cellular	$1.5 \times 10^8$ cells mL <sup>-1</sup>	Fibrin and GelMA	Extrusion-based	Carbopol-based microgels	[98]
	Spheroids	hMSCs	Wholly cellular	n.s.	No	Aspiration-assisted	Carbopol and alginate microparticles	[48]
Cartilage	Spheroids	hASCs	Wholly cellular	n.s.	No	Aspiration-assisted	Alginate	[49]
	Tissue strands	Chondrocytes	Wholly cellular	n.s.	No	Extrusion-based	No	[81]
Vascular	Single cell	HUVECs; hDFs	Quasi-wholly cellular	$4 \times 10^7$ cells mL <sup>-1</sup> $1 \times 10^8$ cells mL <sup>-1</sup>	GelMA	Digital light processing	No	[9]
	Single cell	HUVECs; HDMECs	Quasi-wholly cellular	$2.5 \times 10^7$ cells mL <sup>-1</sup>	Fibrinogen	Droplet-based (piezoelectric)	No	[36]
Vascular and neural	Spheroids and strands (from cell pellets)	hSFs and HUVSMCs	Wholly cellular	n.s.	No	Extrusion-based	Agarose support rods	[52]
	Random aggregates	hiPSCs	Wholly cellular	$2 \times 10^8$ cells mL <sup>-1</sup>	No	Extrusion-based	Collagen–Matrigel	[11]
Neural	Organoids	hiPSCs	Wholly cellular	n.s.	No	Aspiration-assisted (magnetic)	Cellulose nanofibers	[100]
Cardiac	Single cell	hiPSC–CMs and hiPSC–ECs	Quasi-wholly cellular	$1 \times 10^8$ cells mL <sup>-1</sup>	Decellularized extracellular matrix from ormental tissue	Extrusion-based	Alginate microparticles in xanthan gum	[89]
	Spheroids	MSCs; hiPSC–CMs; hCFs	Wholly cellular	n.s.	No	Extrusion-based	Adamantane–hyaluronic acid and cyclodextrin–hyaluronic acid	[47]
Skin	Other shapes	hiPSC–CMs and hNDFs	Quasi-wholly cellular	$2 \times 10^8$ cells mL <sup>-1</sup> (after melting of the sacrificial gelatin layer)	Warmed gelatin	Extrusion-based	No	[85]
	Single cell	hDFs	Quasi-wholly cellular	$3 \times 10^7$ cells mL <sup>-1</sup>	Thrombin and CaCl <sub>2</sub>	Droplet-based (reactive jet impingement)	No	[103]
Intestinal	Single cell	hiSCs	Wholly cellular	$5 \times 10^7$ cells mL <sup>-1</sup>	No	Extrusion-based	Matrigel and collagen	[82]



Regarding living inks formulation, an increasing focus on wholly cellular inks may contribute to avoid concerns regarding possible immunogenic responses and unsynchronous biomaterial degradation, found in conventional scaffold-based approaches.<sup>[40,57,91]</sup> However, the incorporation of minimal fractions of biomaterials into living inks may improve processability by allowing a wide range of cross-linking mechanisms or conferring mechanical support/protection during the printing process. In these strategies, the extent of included biomaterials should not hinder naturally established cell–cell interactions but instead support them. Considering this, both quasi-wholly and wholly cellular formulations have valuable features and have found interesting biomedical applications as above emphasized. As cell surface engineering tools are reaching a spotlight in building block fabrication, higher programmability over cellular interactions and fusion of the living building blocks can be achieved.<sup>[109]</sup> Resorting to these engineered functional building blocks, rapidly assembled tissue mimetics could be obtained in a self-governed/user-defined manner, with improved maturation rates, allowing the faster formation of robust engineered tissues. However, complete tissue maturation comprises cell fusion, cellular (re)organization, and biofunctionality acquisition, which is still required to render tissue-mimetic functions to the designed living constructs. From this standpoint, different building blocks and the corresponding tissues may be associated with different maturation periods, and in the future, its standardization may be valuable to accurately attain mature engineered tissue/organs in a more reproducible manner.

From the current biofabrication technological toolbox, embedded extrusion bioprinting and DLP have shown to be highly compatible and versatile for processing HCD living inks comprised by single cells. On the other hand, as showcased, Kenzan and AAB methodologies are particularly suitable to fabricate HCD constructs using spheroidal building blocks. Other emerging technologies including volumetric bioprinting still require optimizations and upgrades to overcome possible issues regarding structure deposition and light scattering/penetration during cross-linking. We envision that future advances may also arise from other emerging nonlight-based technologies such as 3D bioprinting using ultrasound, which can be highly valuable to overcome some issues regarding cross-linking in HCD across multiple depth scales (>1 cm).<sup>[110,111]</sup>

While moving toward tissue-matched cell densities, the processing of extremely high cell densities imposes inherent challenges at the level of the selection of suitable biofabrication technologies and also at the level of postprinting. If not managed properly, the overall HCD construct may present compromised cell viability which ultimately leads to poor tissue functionality and tissue necrosis, impacting the overall biological performance.<sup>[17,20]</sup> In such cell-dense constructs, a quick exhaustion of nutrients and oxygen may be expected, being the major driver to tissue necrosis. For instance, advancements in tissue oxygenation/vascularization have shown to be crucial to tackling such excessive high-density-related problems by addressing inherent cell nutrition/oxygenation demands of the living constructs. Synergistic advancements in tissue oxygenation/vascularization strategies and biofabrication platforms may contribute to efficiently process higher cell densities, increasing the baseline of current cell densities capable of being processed in

the HCD bioprinting field. Additionally, one must consider other adverse effects arising from the implantation of compromised tissue-like architectures, such as the activation of cell death pathways, consequently leading to phenotypical alterations and triggering of immunogenic responses that may culminate in tissue rejection.<sup>[112,113]</sup> Strategies to ensure cell survival throughout the printed constructs are of utmost importance and may contribute to increasing the baseline of densities suitable for HCD bioprinting.

As the HCD bioprinting field is rapidly progressing and more physiometric engineered tissues are becoming closer to reaching clinical settings, special attention should be given to ethical and regulatory challenges.<sup>[114]</sup> Potential ethical implications can fit into the following categories: i) safety and quality, ii) risks and benefits, iii) informed consent, iv) ownership, v) justice and enhancement, and vi) societal and cultural considerations, as described elsewhere.<sup>[114]</sup> Concurrently, efforts should also focus on ensuring the safety of fabricated constructs, especially by carefully analyzing cell sourcing, as well as their variability and potential long-term effects following implantation.

The successful manufacturing of cell-dense constructs can unlock several applications in regenerative medicine, namely, tissue transplantation, as well as the fabrication of human disease models that can be used for preclinical drug screening or toxicity assays.<sup>[115]</sup> In this sense, the recently described tumor models obtained from spheroid and organoid printing have shown interesting potential to better recapitulate complex intricacies from malignant tissues rendering highly valuable for screening candidate anticancer therapeutics.<sup>[116,117]</sup> Additionally, a more widespread implementation of tissue-mimetic living constructs is envisioned in transplantation/implantation settings, following on the already established strategies for the regeneration of different tissues (i.e., cartilage,<sup>[81]</sup> nerve,<sup>[118]</sup> liver,<sup>[119]</sup> etc.). Owing to the high cell densities found in certain tissues (i.e., heart, brain, etc.), these may benefit from advancements toward HCD biofabrication. Nonetheless, non-cell-dense tissues (e.g., bone, cartilage, skin) may also benefit, since the high number of cells in the generated living constructs can contribute to enhancing and improving de novo matrix deposition as found during tissue development. Hence, following proper in vitro/in situ tissue maturation, it is expected that engineered tissues closely match their native counterpart, presenting similar ECM/cell ratios and functions.<sup>[68,81,98]</sup>

Looking ahead, more advances in HCD 3D bioprinting platforms and cell-rich living inks are expected, and their convergence with other scientific fields, such as developmental biology, computational approaches and in silico design, will eventually culminate into a successful manufacturing pipeline of large-scale engineered living tissue-mimetics with biologically matched functionalities that are suitable for different pre-clinical and clinical applications.

## Acknowledgements

This work was developed within the scope of the project CICECO – Aveiro Institute of Materials, (Grant Nos. UIDB/50011/2020, UIDP/50011/2020, and LA/P/0006/2020), financed by national funds through the FCT/MEC (PIDDAC). The support of the European Research Council for the project REBORN (Grant No. ERC-2019-ADG-883370) is acknowledged. The authors acknowledge the financial support by the Portuguese Foundation

for Science and Technology (FCT) through an Assistant Researcher contract (Grant No. 2022.02106.CEECIND, V.M.G.), and through the doctoral grants (Grant No. 2023.04716.BD, J.A.-P. and Grant No. 2021.08331.BD, B.S.M.).

## Conflict of Interest

The authors declare no conflict of interest.

## Keywords

bioengineering, biofabrication, cellular inks, living constructs, tissue engineering

Received: December 17, 2023

Revised: April 15, 2024

Published online:

- [1] V. M. Gaspar, P. Lavrador, J. Borges, M. B. Oliveira, J. F. Mano, *Adv. Mater.* **2020**, *32*, 1903975.
- [2] S. Guven, P. Chen, F. Inci, S. Tasoglu, B. Erkmen, U. Demirci, *Trends Biotechnol.* **2015**, *33*, 269.
- [3] H.-W. Kang, S. J. Lee, I. K. Ko, C. Kengla, J. J. Yoo, A. Atala, *Nat. Biotechnol.* **2016**, *34*, 312.
- [4] B. D. Cosgrove, K. L. Mui, T. P. Driscoll, S. R. Caliari, K. D. Mehta, R. K. Assoian, J. A. Burdick, R. L. Mauck, *Nat. Mater.* **2016**, *15*, 1297.
- [5] B. A. Yang, T. M. Westerhof, K. Sabin, S. D. Merajver, C. A. Aguilar, *Adv. Sci.* **2021**, *8*, 2002825.
- [6] T. Lecuit, A. S. Yap, *Nat. Cell Biol.* **2015**, *17*, 533.
- [7] M. Grellier, L. Bordenave, J. Amédée, *Trends Biotechnol.* **2009**, *27*, 562.
- [8] U. Blache, M. M. Stevens, E. Gentleman, *Nat. Biomed. Eng.* **2020**, *4*, 357.
- [9] S. You, Y. Xiang, H. H. Hwang, D. B. Berry, W. Kiratitanaporn, J. Guan, E. Yao, M. Tang, Z. Zhong, X. Ma, D. Wangpraseurt, Y. Sun, T. Y. Lu, S. Chen, *Sci. Adv.* **2023**, *9*, eade7923.
- [10] L. Kocgozlu, T. B. Saw, A. P. Le, I. Yow, M. Shagirov, E. Wong, R.-M. Mège, C. T. Lim, Y. Toyama, B. Ladoux, *Curr. Biol.* **2016**, *26*, 2942.
- [11] D. L. L. Ho, S. Lee, J. Du, J. D. Weiss, T. Tam, S. Sinha, D. Klingner, S. Devine, A. Hamfeldt, H. T. Leng, J. E. Herrmann, M. He, L. G. Fradkin, T. K. Tan, D. Standish, P. Tomasello, D. Traul, N. Dianat, R. Ladi, Q. Vicard, K. Katikireddy, M. A. Skylar-Scott, *Adv. Healthcare Mater.* **2022**, *11*, 2201138.
- [12] R. E. McClelland, R. Dennis, L. M. Reid, J. P. Stegemann, B. Palsson, J. M. Macdonald, *Introduction to Biomedical Engineering*, Elsevier Inc, Amsterdam **2012**, pp. 273–357.
- [13] P. Lavrador, V. M. Gaspar, J. F. Mano, *EBioMedicine* **2021**, *74*, 103717.
- [14] J. M. Unagolla, A. C. Jayasuriya, *Appl. Mater. Today* **2020**, *18*, 100479.
- [15] M. A. Skylar-Scott, S. G. M. Uzel, L. L. Nam, J. H. Ahrens, R. L. Truby, S. Damaraju, J. A. Lewis, *Sci. Adv.* **2019**, *5*, eaaw2459.
- [16] A. Y. Chen, C. Zhong, T. K. Lu, *ACS Synth. Biol.* **2015**, *4*, 8.
- [17] J. Karvinen, M. Kellomäki, *Int. J. Bioprint.* **2023**, *32*, e00274.
- [18] K. Shariati, A. S. Ling, S. Fuchs, B. Dillenburger, W. Liu, M. Ma, *Adv. Funct. Mater.* **2022**, *32*, 2108057.
- [19] K. L. Miller, Y. Xiang, C. Yu, J. Pustelnik, J. Wu, X. Ma, T. Matsui, K. Imahashi, S. Chen, *Organs-on-a-Chip* **2021**, *3*, 100007.
- [20] G. Cidonio, M. Glinka, J. I. Dawson, R. O. C. Oreffo, *Biomaterials* **2019**, *209*, 10.
- [21] G. E. Neurohr, A. Amon, *Trends Cell Biol.* **2020**, *30*, 213.
- [22] M. A. Heinrich, W. Liu, A. Jimenez, J. Yang, A. Akpek, X. Liu, Q. Pi, X. Mu, N. Hu, R. M. Schifferers, J. Prakash, J. Xie, Y. S. Zhang, *Small* **2019**, *15*, 1805510.
- [23] K. J. Wolf, J. D. Weiss, S. G. M. Uzel, M. A. Skylar-Scott, J. A. Lewis, *Cell Stem Cell* **2022**, *29*, 667.
- [24] Y. Ren, X. Yang, Z. Ma, X. Sun, Y. Zhang, W. Li, H. Yang, L. Qiang, Z. Yang, Y. Liu, C. Deng, L. Zhou, T. Wang, J. Lin, T. Li, T. Wu, J. Wang, *Int. J. Bioprint.* **2021**, *7*, 18.
- [25] S. V. Murphy, A. Atala, *Nat. Biotechnol.* **2014**, *32*, 773.
- [26] N. Khoshnood, A. Zamanian, *Int. J. Bioprint.* **2020**, *19*, e00088.
- [27] P. S. Gungor-Ozkerim, I. Inci, Y. S. Zhang, A. Khademhosseini, M. R. Dokmeci, *Biomater. Sci.* **2018**, *6*, 915.
- [28] D. Banerjee, Y. P. Singh, P. Datta, V. Ozbolat, A. O'Donnell, M. Yeo, I. T. Ozbolat, *Biomaterials* **2022**, *291*, 121881.
- [29] J. Laurent, G. Blin, F. Chatelain, V. Vanneaux, A. Fuchs, J. Larghero, M. Théry, *Nat. Biomed. Eng.* **2017**, *1*, 939.
- [30] N. I. Moldovan, N. Hibino, K. Nakayama, *Tissue Eng., Part B* **2017**, *23*, 237.
- [31] W. L. Ng, J. M. Lee, W. Y. Yeong, M. W. Naing, *Biomater. Sci.* **2017**, *5*, 632.
- [32] H. Gudapati, M. Dey, I. Ozbolat, *Biomaterials* **2016**, *102*, 20.
- [33] R. D. Pedde, B. Mirani, A. Navai, T. Styan, S. Wong, M. Mehrli, A. Thakur, N. K. Mohtaram, A. Bayati, A. Dolatshahi-Pirouz, M. Nikkhah, S. M. Willerth, M. Akbari, *Adv. Mater.* **2017**, *29*, 1606061.
- [34] C. Mandrycky, Z. Wang, K. Kim, D.-H. Kim, *Biotechnol. Adv.* **2016**, *34*, 422.
- [35] R. da Conceicao Ribeiro, D. Pal, A. M. Ferreira, P. Gentile, M. Benning, K. Dalgarno, *Biofabrication* **2019**, *11*, 015014.
- [36] K. Tröndle, F. Koch, G. Finkenzeller, G. B. Stark, R. Zengerle, P. Koltay, S. Zimmermann, *J. Tissue Eng. Regen. Med.* **2019**, *13*, 1883.
- [37] A. D. Graham, S. N. Olof, M. J. Burke, J. P. K. Armstrong, E. A. Mikhailova, J. G. Nicholson, S. J. Box, F. G. Szele, A. W. Perriman, H. Bayley, *Sci. Rep.* **2017**, *7*, 7004.
- [38] W. Zhu, X. Ma, M. Gou, D. Mei, K. Zhang, S. Chen, *Curr. Opin. Biotechnol.* **2016**, *40*, 103.
- [39] R. Chang, J. Nam, W. Sun, *Tissue Eng., Part A* **2008**, *14*, 41.
- [40] O. Jeon, Y. Bin Lee, H. Jeong, S. J. Lee, D. Wells, E. Alsberg, *Mater. Horiz.* **2019**, *6*, 1625.
- [41] J. Madrid-Wolff, A. Boniface, D. Loterie, P. Delrot, C. Moser, *Adv. Sci.* **2022**, *9*, 2105144.
- [42] J. Guan, S. You, Y. Xiang, J. Schimelman, J. Alido, X. Ma, M. Tang, S. Chen, *Biofabrication* **2022**, *14*, 015011.
- [43] J. T. Toombs, M. Luitz, C. C. Cook, S. Jenne, C. C. Li, B. E. Rapp, F. Kotz-Helmer, H. K. Taylor, *Science* **2022**, *376*, 308.
- [44] P. N. Bernal, M. Bouwmeester, J. Madrid-Wolff, M. Falandt, S. Florczak, N. G. Rodriguez, Y. Li, G. Größbacher, R. Samsom, M. van Wolferen, L. J. W. van der Laan, P. Delrot, D. Loterie, J. Malda, C. Moser, B. Spee, R. Levato, *Adv. Mater.* **2022**, *34*, 2110054.
- [45] D. Murata, K. Arai, K. Nakayama, *Adv. Healthcare Mater.* **2020**, *9*, 1901831.
- [46] B. Ayan, D. N. Heo, Z. Zhang, M. Dey, A. Povilianskas, C. Drapaca, I. T. Ozbolat, *Sci. Adv.* **2020**, *6*, 10.
- [47] A. C. Daly, M. D. Davidson, J. A. Burdick, *Nat. Commun.* **2021**, *12*, 753.
- [48] B. Ayan, N. Celik, Z. Zhang, K. Zhou, M. H. Kim, D. Banerjee, Y. Wu, F. Costanzo, I. T. Ozbolat, *Commun. Phys.* **2020**, *3*, 183.
- [49] B. Ayan, Y. Wu, V. Karuppagounder, F. Kamal, I. T. Ozbolat, *Sci. Rep.* **2020**, *10*, 13148.
- [50] I. T. Ozbolat, Y. Yu, *IEEE Trans. Biomed. Eng.* **2013**, *60*, 691.
- [51] A. R. Verissimo, K. Nakayama, in *3D Printing and Biofabrication*, (Eds: A. Ovsianikov, J. Yoo, V. Mironov), Springer International Publishing, Cham **2017**, pp. 1–20.
- [52] C. Norotte, F. S. Marga, L. E. Niklason, G. Forgacs, *Biomaterials* **2009**, *30*, 5910.

- [53] I. N. Aguilar, L. J. Smith, D. J. Olivos, T. M. G. Chu, M. A. Kacena, D. R. Wagner, *Int. J. Bioprint.* **2019**, *15*, e00048.
- [54] C. Kropp, D. Massai, R. Zweigerdt, *Process Biochem.* **2017**, *59*, 244.
- [55] D. B. Kolesky, R. L. Truby, A. S. Gladman, T. A. Busbee, K. A. Homan, J. A. Lewis, *Adv. Mater.* **2014**, *26*, 3124.
- [56] P. Wu, H. Asada, M. Hakamada, M. Mabuchi, *Adv. Mater.* **2023**, *35*, 2209149.
- [57] V. Mironov, R. P. Visconti, V. Kasyanov, G. Forgacs, C. J. Drake, R. R. Markwald, *Biomaterials* **2009**, *30*, 2164.
- [58] E. Mirdamadi, J. W. Tashman, D. J. Shiwarski, R. N. Palchesko, A. W. Feinberg, *ACS Biomater. Sci. Eng.* **2020**, *6*, 6453.
- [59] S. Grebenyuk, A. R. Abdel Fattah, M. Kumar, B. Toprakhisar, G. Rustandi, A. Vananroye, I. Salmon, C. Verfaillie, M. Grillo, A. Ranga, *Nat. Commun.* **2023**, *14*, 193.
- [60] T. Agarwal, S. Kazemi, M. Costantini, F. Perfeito, C. R. Correia, V. Gaspar, L. Montazeri, C. De Maria, J. F. Mano, M. Vosough, P. Makvandi, T. K. Maiti, *Mater. Sci. Eng., C* **2021**, *122*, 111896.
- [61] M. Gholipourmalekabadi, S. Zhao, B. S. Harrison, M. Mozafari, A. M. Seifalian, *Trends Biotechnol.* **2016**, *34*, 1010.
- [62] M. Touri, F. Moztarzadeh, N. A. A. Osman, M. M. Dehghan, M. Mozafari, *Mater. Sci. Eng., C* **2018**, *84*, 236.
- [63] C. Y. C. Montesdeoca, S. Afewerki, T. D. Stocco, M. A. F. Corat, M. M. M. de Paula, F. R. Marciano, A. O. Lobo, *Colloids Surf., B* **2020**, *194*, 111192.
- [64] S. Wang, J. Qiu, A. Guo, R. Ren, W. He, S. Liu, Y. Liu, *J. Nanobiotechnol.* **2020**, *18*, 84.
- [65] P. S. Patil, M. Mansouri, N. D. Leipzig, *Adv. Biosyst.* **2020**, *4*, 1900250.
- [66] A. Farzin, S. Hassan, L. S. Moreira Teixeira, M. Gurian, J. F. Crispim, V. Manhas, A. Carlier, H. Bae, I. Geris, I. Noshadi, S. R. Shin, J. Leijten, *Adv. Funct. Mater.* **2021**, *31*, 2100850.
- [67] I. Lee, A. Surendran, S. Fleury, I. Gimino, A. Curtiss, C. Fell, D. J. Shiwarski, O. Refy, B. Rothrock, S. Jo, T. Schwartzkopff, A. S. Mehta, Y. Wang, A. Sipe, S. John, X. Ji, G. Nikiforidis, A. W. Feinberg, J. Hester, D. J. Weber, O. Veiseh, J. Rivnay, T. Cohen-Karni, *Nat. Commun.* **2023**, *14*, 7019.
- [68] D. N. Heo, B. Ayan, M. Dey, D. Banerjee, H. Wee, G. S. Lewis, I. T. Ozbolat, *Biofabrication* **2021**, *13*, 015013.
- [69] L. Song, X. Yuan, Z. Jones, K. Griffin, Y. Zhou, T. Ma, Y. Li, *Sci. Rep.* **2019**, *9*, 5977.
- [70] I. Papantoniou, Y. Guyot, M. Sonnaert, G. Kerckhofs, F. P. Luyten, L. Geris, J. Schrooten, *Biotechnol. Bioeng.* **2014**, *111*, 2560.
- [71] J. Schmid, S. Schwarz, R. Meier-Staude, S. Sudhop, H. Clausen-Schaumann, M. Schieker, R. Huber, *Tissue Eng., Part C* **2018**, *24*, 585.
- [72] R. F. Canadas, Z. Liu, L. Gasperini, D. C. Fernandes, F. R. Maia, R. L. Reis, A. P. Marques, C. Liu, J. M. Oliveira, *Biofabrication* **2022**, *14*, 025022.
- [73] J. Chakraborty, S. Chawla, S. Ghosh, *Curr. Opin. Biotechnol.* **2022**, *78*, 102832.
- [74] F. van Roy, G. Bex, *Cell. Mol. Life Sci.* **2008**, *65*, 3756.
- [75] B. Nzigou Mombo, B. M. Bijonowski, C. A. Raab, S. Niland, K. Brockhaus, M. Müller, J. A. Eble, S. V. Wegner, *Nat. Commun.* **2023**, *14*, 6292.
- [76] E. Cachat, W. Liu, K. C. Martin, X. Yuan, H. Yin, P. Hohenstein, J. A. Davies, *Sci. Rep.* **2016**, *6*, 20664.
- [77] S. G. Patrício, L. R. Sousa, T. R. Correia, V. M. Gaspar, L. S. Pires, J. L. Luís, J. M. Oliveira, J. F. Mano, *Biofabrication* **2020**, *12*, 035017.
- [78] K. Nagahama, Y. Kimura, A. Takemoto, *Nat. Commun.* **2018**, *9*, 2195.
- [79] N. Ueda, S. Sawada, F. Yuasa, K. Kato, K. Nagahama, *ACS Appl. Mater. Interfaces* **2022**, *14*, 52618.
- [80] Y. Kimura, S. Aoyama, N. Ueda, T. Katayama, K. Ono, K. Nagahama, *Adv. Biol.* **2021**, *5*, 2000106.
- [81] Y. Yu, K. K. Moncal, J. Li, W. Peng, I. Rivero, J. A. Martin, I. T. Ozbolat, *Sci. Rep.* **2016**, *6*, 28714.
- [82] J. A. Brassard, M. Nikolaev, T. Hübscher, M. Hofer, M. P. Lutolf, *Nat. Mater.* **2021**, *20*, 22.
- [83] M. R. Blatchley, K. S. Anseth, *Nat. Rev. Bioeng.* **2023**, *1*, 329.
- [84] A. Akkouch, Y. Yu, I. T. Ozbolat, *Biofabrication* **2015**, *7*, 031002.
- [85] J. H. Ahrens, S. G. M. Uzel, M. Skylar-Scott, M. M. Mata, A. Lu, K. T. Kroll, J. A. Lewis, *Adv. Mater.* **2022**, *34*, 2200217.
- [86] A. Alblawi, A. S. Ranjani, H. Yasmin, S. Gupta, A. Bit, M. Rahimi-Gorji, *Comput. Methods Programs Biomed.* **2020**, *185*, 105148.
- [87] N. I. Moldovan, *J. Cell. Mol. Med.* **2018**, *22*, 2964.
- [88] G. Gao, Y. Huang, A. F. Schilling, K. Hubbell, X. Cui, *Adv. Healthcare Mater.* **2018**, *7*, 1701018.
- [89] N. Noor, A. Shapira, R. Edri, I. Gal, L. Wertheim, T. Dvir, *Adv. Sci.* **2019**, *6*, 1900344.
- [90] B. S. Moura, M. V. Monteiro, L. P. Ferreira, P. Lavrador, V. M. Gaspar, J. F. Mano, *Adv. Funct. Mater.* **2022**, *32*, 2202825.
- [91] D. F. Williams, *Biomaterials* **2008**, *29*, 2941.
- [92] M. H. Kim, D. Banerjee, N. Celik, I. T. Ozbolat, *Biofabrication* **2022**, *14*, 024103.
- [93] I. A. Hatton, E. D. Galbraith, N. S. C. Merleau, T. P. Miettinen, B. M. Smith, J. A. Shander, *Proc. Natl. Acad. Sci. USA* **2023**, *120*, 2017.
- [94] K. Jakab, C. Norotte, F. Marga, K. Murphy, G. Vunjak-Novakovic, G. Forgacs, *Biofabrication* **2010**, *2*, 022001.
- [95] M. W. Laschke, M. D. Menger, *Biotechnol. Adv.* **2017**, *35*, 782.
- [96] M. C. Decarli, R. Amaral, D. P. dos Santos, L. B. Tofani, E. Katayama, R. A. Rezende, J. V. L. da Silva, K. Swiech, C. A. T. Suazo, C. Mota, L. Moroni, A. M. Moraes, *Biofabrication* **2021**, *13*, 032002.
- [97] M. C. Decarli, A. Seijas-Gamardo, F. L. C. Morgan, P. Wieringa, M. B. Baker, J. V. L. Silva, A. M. Moraes, L. Moroni, C. Mota, *Adv. Healthcare Mater.* **2023**, *12*, 2203021.
- [98] Y. Fang, M. Ji, B. Wu, X. Xu, G. Wang, Y. Zhang, Y. Xia, Z. Li, T. Zhang, W. Sun, Z. Xiong, *ACS Appl. Mater. Interfaces* **2023**, *15*, 43492.
- [99] H. Clevers, *Cell* **2016**, *165*, 1586.
- [100] J. G. Roth, L. G. Brunel, M. S. Huang, Y. Liu, B. Cai, S. Sinha, F. Yang, S. P. Paçca, S. Shin, S. C. Heilshorn, *Nat. Commun.* **2023**, *14*, 4346.
- [101] J. A. Brassard, M. P. Lutolf, *Cell Stem Cell* **2019**, *24*, 860.
- [102] M. Hofer, M. P. Lutolf, *Nat. Rev. Mater.* **2021**, *6*, 402.
- [103] M. Kotlarz, A. M. Ferreira, P. Gentile, S. J. Russell, K. Dalgarno, *Bio-Des. Manuf.* **2022**, *5*, 512.
- [104] S. Y. Hann, H. Cui, T. Esworthy, S. Miao, X. Zhou, S. Lee, J. P. Fisher, L. G. Zhang, *Transl. Res.* **2019**, *217*, 46.
- [105] J. Zhang, P. Byers, A. Erben, C. Frank, L. Schulte-Spechtel, M. Heymann, D. Docheva, H. P. Huber, S. Sudhop, H. Clausen-Schaumann, *Adv. Funct. Mater.* **2021**, *31*, 2100066.
- [106] C. Trentesaux, T. Yamada, O. D. Klein, W. A. Lim, *Cell Stem Cell* **2023**, *30*, 10.
- [107] M. Tanaka, S. M. Montgomery, L. Yue, Y. Wei, Y. Song, T. Nomura, H. J. Qi, *Sci. Adv.* **2023**, *9*, 6.
- [108] S. Janbaz, C. Coulais, *Nat. Commun.* **2024**, *15*, 1255.
- [109] J. Almeida-Pinto, M. R. Lagarto, P. Lavrador, J. F. Mano, V. M. Gaspar, *Adv. Sci.* **2023**, *10*, 2304040.
- [110] L. Debbi, M. Machour, D. Dahis, H. Shoyhet, M. Shuhmaher, R. Potter, Y. Tabori, I. Goldfracht, I. Dennis, T. Blechman, T. Fuchs, H. Azhari, S. Levenberg, *Small Methods* **2024**, 2301197.
- [111] X. Kuang, Q. Rong, S. Belal, T. Vu, A. M. López, N. Wang, M. O. Arcan, C. E. Garciamendez-Mijares, M. Chen, J. Yao, Y. S. Zhang, *Science* **2023**, *382*, 1148.
- [112] J. Belizário, L. Vieira-Cordeiro, S. Enns, *Mediators Inflammation* **2015**, *2015*, 128076.
- [113] W. Park, S. Wei, B.-S. Kim, B. Kim, S.-J. Bae, Y. C. Chae, D. Ryu, K.-T. Ha, *Exp. Mol. Med.* **2023**, *55*, 1573.
- [114] P. Datta, L. Y. Cabrera, I. T. Ozbolat, *Trends Biotechnol.* **2023**, *41*, 6.
- [115] P. Datta, A. Barui, Y. Wu, V. Ozbolat, K. K. Moncal, I. T. Ozbolat, *Biotechnol. Adv.* **2018**, *36*, 1481.

- [116] D. Hakobyan, C. Médina, N. Dusserre, M.-L. Stachowicz, C. Handschin, J.-C. Fricain, J. Guillermet-Guibert, H. Oliveira, *Biofabrication* **2020**, *12*, 035001.
- [117] M. Dey, M. H. Kim, M. Dogan, M. Nagamine, L. Kozhaya, N. Celik, D. Unutmaz, I. T. Ozbolat, *Adv. Funct. Mater.* **2022**, *32*, 2203966.
- [118] S. Mitsuzawa, R. Ikeguchi, T. Aoyama, H. Takeuchi, H. Yurie, H. Oda, S. Ohta, M. Ushimaru, T. Ito, M. Tanaka, Y. Kunitomi, M. Tsuji, S. Akieda, K. Nakayama, S. Matsuda, *Cell Transplant.* **2019**, *28*, 1231.
- [119] Y. Yanagi, K. Nakayama, T. Taguchi, S. Enosawa, T. Tamura, K. Yoshimaru, T. Matsuura, M. Hayashida, K. Kohashi, Y. Oda, T. Yamaza, E. Kobayashi, *Sci. Rep.* **2017**, *7*, 14085.



**José Almeida-Pinto** holds a M.Sc. in Molecular Biotechnology and Bioengineering. Currently, he is a Ph.D. student in Medical Biotechnology at the COMPASS Research Group based in the Associate Laboratory CICECO – Aveiro Institute of Materials. His research interests include metabolic glyco-engineering and synthetic biology tools, as well as the application of these precise technologies for bottom-up tissue engineering and fabrication of 3D/4D mammalian living materials.



**Beatriz S. Moura** holds a M.Sc. in Bioengineering, with a specialization in Molecular Biotechnology. Currently, she is a Ph.D. student in Biotechnology at the COMPASS Research Group, in the Associate Laboratory CICECO – Aveiro Institute of Materials. She is focusing her work on developing organoids and responsive living materials with high cellular density, both for tissue engineering and cancer disease modeling platforms, applying innovative technologies such as 3D bioprinting, and the use of decellularized matrix hydrogels as highly biomimetic-tissue-derived matrixes, where such platforms will be developed.



**Vítor M. Gaspar** is an Assistant Professor at the Department of Chemistry of the University of Aveiro and member of COMPASS Research Group at CICECO – Aveiro Institute of Materials. His research focuses on exploring the precision chemical modification of ECM-biomimetic and tissue-derived biomaterials, particularly decellularized extracellular matrix, with a special emphasis on their use for bottom-up engineering of cell–biomaterial living microtissues and organoids. He is also exploring advanced manufacturing techniques for processing cell surfaces to generate living architectures for tissue engineering and in vitro disease modeling applications.





**João F. Mano** is a Full Professor at the Department of Chemistry of the University of Aveiro, Portugal, and Director of the COMPASS Research Group from the Associate Laboratory CICECO – Aveiro Institute of Materials. His research focuses on applying biomimetic and nano/micro-technology approaches to polymer-based biomaterials and surfaces to develop biomedical devices with improved structural and (multi)functional properties, or in the engineering of microenvironments to control cell behavior and organization, to be exploited clinically in advanced therapies or for drug screening.